



DYNAMIC SHOCK ABSORBER

A Major Qualifying Project Report

Submitted to the Faculty
of

WORCESTER POLYTECHNIC INSTITUTE
Worcester, Massachusetts, U.S.A

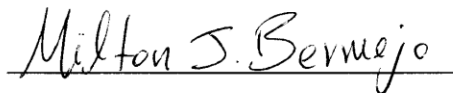
in partial fulfillment of the requirements for the

Degree of Bachelor of Science

on the date of

March 17th, 2009

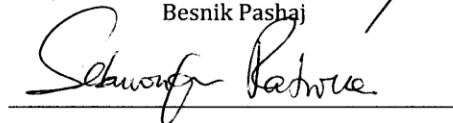
by



Milton J. Bermejo Calle



Besnik Pashaj



Patrick Sebuwufu



Prof. Alexander E. Emmanuel

ADVISOR

Abstract

The objective of this project was to design a dynamic suspension system that minimizes the vertical oscillations of the vehicle's body regardless of different road conditions. A series of five modules were designed to achieve this goal. The modules generate a force similar to the effects of an uneven road that creates oscillations in the vehicle's body. The vertical velocity of the body was calculated and processed through a controller to achieve the required signal to suppress these oscillations. This process was implemented through the use of electromagnetic circuitry.

Executive Summary

The main goal of this project is to design a superior suspension system for the automobile market. Due to the restrictions of the common vehicle suspensions systems, there is a need for a more reliable and efficient systems. Our research shows that there exist active suspensions systems that adapt to the road conditions instantaneously and are highly efficient but are also high in cost. Due to these factors we created a new suspensions system that uses dynamic electromagnetic shock absorbers. The system performance is efficient, affordable and performs the tasks established by the goals of this project.

The mechanism and theory of the current suspensions system was analyzed to achieve a better understanding. A mechanical representation of a suspension system was designed based on these analyses. Coils and magnets were incorporate in the design of this model necessary to achieve an electromagnetic shock absorber. The dynamic equations of the system were derived using this model and Newton's laws. These equations represent the reaction of the suspension system to the inconsistency of the road. Through them the equivalent electrical circuit of the suspension system was drawn. Analysis of this circuit was done using the PSPICE simulation program to achieve a better understanding of how a suspension system reacts to different types of road conditions. These analyses were essential to determine the necessary reforms that the circuit needed to achieve constant stability. The information was used to design a new electrical circuit that represents our dynamic electromagnetic suspension system.

This circuit helped us identify the necessary modules to achieve our desired results. These modules were represented in a block diagram to better understand the composition of the system and the necessary steps required. There are four main modules in the block diagram shown in Figure i: Detailed Block Diagram: Road Condition, Signal Conditioning, Controller, Current Driver and the AC to DC Converter. The road condition module is used to simulate the different conditions encountered on the road. Through the use of an oscillator and a transistor a triangular wave current was produced that gave the model a certain movement to a desired frequency. The signal conditioning module will record the acceleration of the model and represent it as a voltage signal. With the use of an integrator

circuit the signal will be converted to give the model's velocity. This is then used in the controller module where it is modified to drive an H-Bridge. The modifications of the signal include amplification, integration and pulse width modulation. The H-Bridge is connected to the damper coil and the signal that it supplies is responsible for attaining constant displacement of the model (automobile's body). The circuitry of some of these modules requires to be supplied with DC voltage. In this case the AC-to-DC converter module is used to change the AC voltage that is supplied by the wall outlet to a required DC voltage. The description of each individual module includes circuit design, analysis and simulation with the help of programs such as MULTISIM and PSPICE. Also included are the physical requirements of each individual module and their prototypes.

The simulation results obtained for the overall system were positive and the system seems to behave almost as desired. The following report outlines more detail descriptions of the design process and results obtained for the dynamic electromagnetic suspension system of an automobile.

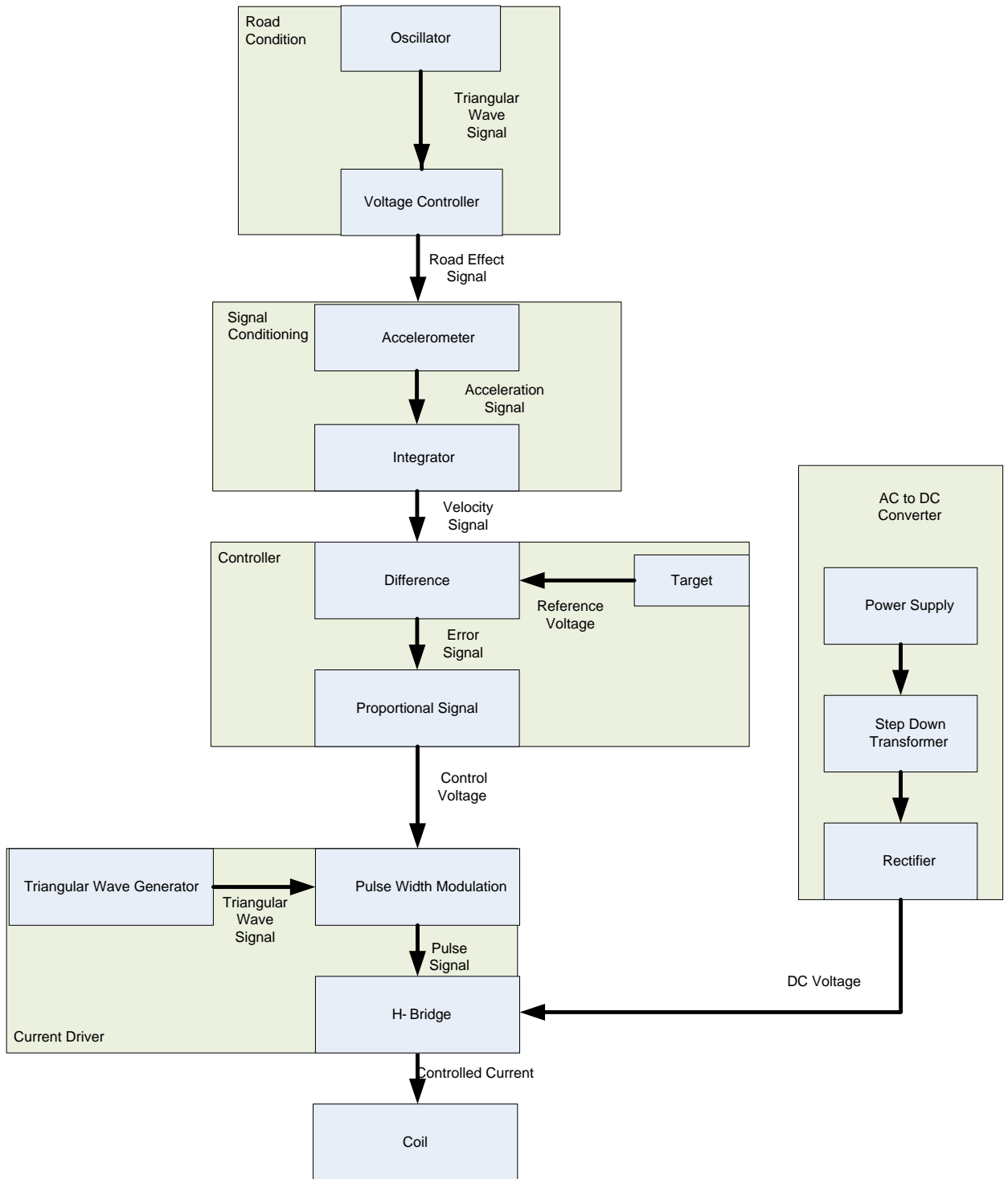


Figure i: Detailed Block Diagram

Table of Contents

Abstract.....	1
Executive Summary.....	2
Table of Figures.....	6
Introduction	8
1. Electrical Transformation of the Suspension System	10
2. System Design: Block Diagram.....	18
3. Road Condition Module	19
3.1 Prior Art Research	19
3.2 Road Condition Block Diagram	23
3.2.1 Oscillator Design	24
3.2.2 Voltage Controlled Source Design	30
4. Signal Conditioning	35
4.1. Accelerometer.....	35
4.2. Integrator	38
5. Controller	43
5.1. Difference Amplifier.....	45
5.2. Proportional Amplifier	47
6. Current Driver	52
6.1. Triangular Wave Oscillator.....	52
6.2. Pulse Width Modulation	55
6.3. H-Bridge	57
7. AC to DC Converter	61
7.1. Transformer and Rectifier.....	62
8. Conclusion.....	68
9. Bibliography	70
APPENDIX A1: SCHEMATICS.....	72
APPENDIX B. PSPICE CODE	73
APPENDIX C: DATASHEETS.....	76

Table of Figures

Figure 1.1: Shock Absorber (2).....	10
Figure 1.2: Generic Suspension System representation	11
Figure 1.3: Mechanical Representation of New Suspension System.....	11
Figure 1.4: Free Body Diagrams of System	13
Figure 1.5: Electrical Representation of the Suspension System.....	14
Figure 1.6: Step Input signal $F(t)$ and Current through Inductor $M_b Y$	15
Figure 1.7: Impulse Input Signal $V(1) [F(t)]$ and Current through Inductor $M_b I(Lmb) [Y]$	16
Figure 1.8: Current through M_b with Respect to Frequency.....	17
Figure 2.1: Overall Block Diagram.....	18
Figure 3.1: Road Condition and Its Corresponding Connections	19
Figure 3.2: Digital Controlled Sine Wave Generator (3)	20
Figure 3.3: Generic Triangular Wave Generator	21
Figure 3.4: Schmitt Trigger Circuit and its Output	22
Figure 3.5: Integrator circuit and its output	22
Figure 3.6: Triangular Wave Generator and its Outputs.....	23
Figure 3.7: Road Condition Block Diagram	23
Figure 3.8: Final Triangular Wave Generator Schematic	24
Figure 3.9: Wave Generator Simulation Outputs of Node-4 & Node-V7	26
Figure 3.10: Min Frequency when $R_2 = 5K\Omega$ and Max Frequency when $R_2 = 0\Omega$	26
Figure 3.11; Varying Amplitude at Min & Max Frequency	27
Figure 3.12: TL082 op-amp (4).....	28
Figure 3.13: Characteristics of TL082 op-amp (4)	28
Figure 3.14: Triangular Wave Generator Circuit.....	29
Figure 3.15: Oscillator at Maximum and Minimum Frequency	29
Figure 3.16: Oscillator at a Random Frequency.....	30
Figure 3.17: Voltage Controlled Schematic and Its Corresponding Connections	30
Figure 3.18: Comparison of voltages V_z and V_L (6)	31
Figure 3.19: Input and Output Signals of the Voltage Controlled Source at Minimum Frequency	32
Figure 3.20: Input and Output Signals of the Voltage Control Source at Maximum Frequency	33
Figure 3.21: QM50DY-2H transistor (6)	33
Figure 3.22: Characteristics of the transistor (6)	34
Figure 3.23: Voltage Control Source Circuit.....	34
Figure 4.1: Block Diagram of the Signal Conditioning Module	35
Figure 4.2: Accelerometer (7)	36
Figure 4.3: Accelerator Output Signal.....	37
Figure 4.4: Integrator Circuit.....	38
Figure 4.5: Magnitude Plot of the Frequency Response.....	39
Figure 4.6: Phase Plot of the Frequency Response.....	40
Figure 4.7: Input and Output Signals of the Integrator at 10Hz Frequency	40

Figure 4.8: Input and Output Signal of Integrator at 0.8Hz Frequency	41
Figure 4.9: Input and Output Signal of Integrator at 5Hz Frequency	42
Figure 5.1 Electrical Representation of Suspension System	43
Figure 5.2: Controller	44
Figure 5.3: Block Diagram of Controller	44
Figure 5.4: Velocities (\dot{Y}) I(Lmb) and (\dot{X}) I(Lms) due to Force F(t) (V(1))	46
Figure 5.5: Proportional Amplifier Circuit	47
Figure 5.6: Vertical Velocity \dot{Y} of Vehicle's Body	48
Figure 5.7: Input Voltage V(1) (F(t)) and Currents through Ms I(Lms) and Mb I(Lmb)	49
Figure 5.8: Suspension System Signals at 0.2Hz Frequency	49
Figure 5.9: Suspension System Signals at 2.7 Hz Resonance Frequency	50
Figure 5.10: Suspension system at 20 Hz Frequency	50
Figure 5.11: Analog Representation of Controller Module	51
Figure 6.1: Current Driver Block Diagram	52
Figure 6.2: Triangular Wave Generator	53
Figure 6.3: 555-Timer Output	54
Figure 6.4: Output of Triangular Wave Oscillator	55
Figure 6.5: Schematic of PWM Module	55
Figure 6.6: Output and Input Signal of the PWM	57
Figure 6.7: H-Bridge Circuit	57
Figure 6.8: H-Bridge Connections using the Darlington BJTs	58
Figure 6.9: Control Signal V(control) and Control Current of damper coil	60
Figure 7.1: AC-to-DC converter Block Diagram	61
Figure 7.2: POWERSTAT Transformer	62
Figure 7.3: Rating Chart of POWERSTAT (9)	63
Figure 7.4: Rectifier Circuit	63
Figure 7.5: AC-to-DC Converter	66
Figure 7.6: Output Voltage of the AC-to-DC Converter	66
Figure 7.7: Output Current of the AC-to-DC Converter	67

Introduction

There are different components that make the automobile performance reliable and secure for the driver. Even though the customer is attracted to how powerful the car is or how fast it can go, it would be nothing if the driver couldn't control the car. That is why a reliable suspension system is crucial in the engineering of a vehicle. The important tasks that this systems should accomplish is to support the vehicle weight, isolate the body from the vibrations caused by the unevenness of the road and keep a firm contact between the tires and the road. Most suspension systems are composed of springs and dampers which limit the systems performance due to their physical constraints. These restrictions apply to the systems parameters which are fixed and are chosen on the typical operation of the vehicle and the safety of the passengers. Therefore the quality of the vehicle comfort is restricted.

To resolve these problems different types of suspension systems have been created. The most reliable are the active suspensions systems. These systems adapt to the road conditions instantaneously due to the use of sensors. Microcontrollers are also used to store the control gains corresponding to various conditions of the road. Although they are highly efficient, the use of these systems is limited to few expensive models due to their high price. There are also medians of these two suspension systems that are less expensive. In these semi-active systems, an active force generator is replaced by a damper that can vary its characteristic with sufficient speed. However these systems are not adapted for low frequency inputs as well as braking, accelerations and cornering maneuvers.

This paper deals with a new suspension system that uses a dynamic electromagnetic shock absorber. With the use of electronic circuits, the system will analyze the wheel's movement and adapt the vehicle to maintain constant stability. In effect, the vehicle's body will stay at the same vertical position at all times regardless of the road conditions. This system is a modification of the suspension system already used by the vehicle. If the electrical circuitry loses power or has a malfunction, the regular suspension system will work normally. Analysis of the behavior of this system is done using a variety of changes in

the parameters to achieve maximum efficiency. This model is applied to each individual shock absorber. This paper provides in details with the behavior of this system in different types of road conditions to assure its efficiency and reliability. The system will have a low cost and will be controllable. (1)

1. Electrical Transformation of the Suspension System

The mechanism of a generic shock absorber is shown in Figure 1.1 . The components of the shock absorber are attached at the end of a piston rod that works against the hydraulic fluid of the pressure tube. While the suspension system moves up and down the hydraulic fluid is forced through tiny holes inside the piston creating a damping effect on the movement. This will reduce the speed of the piston which as a result will slow down the springs and the suspension movement reducing the effect of these vibrations on the vehicle's body. (2)

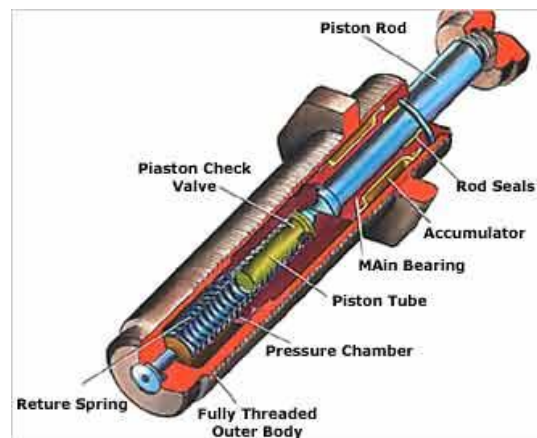


Figure 1.1: Shock Absorber (2)

This concept is applied to the construction of a new model. Analysis and construction will be done for only one wheel of the suspension systems to simplify the problem to a one dimensional spring-damper system. The diagram of a general suspension system is shown in Figure 1.2.

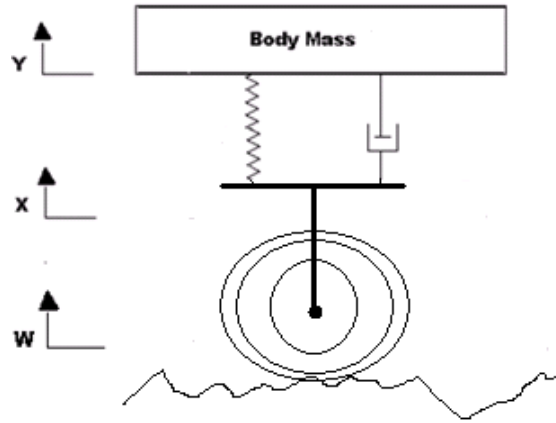


Figure 1.2: Generic Suspension System representation

The suspension system is represented in relation to the spring's constants (K_1 and K_2), damping coefficients (d_1 and d_2) and masses of the body and suspension system (M_b and M_s). The new model was drawn and built based on this representation. The Figure 1.3 shows the mechanical representation of the model with its components.

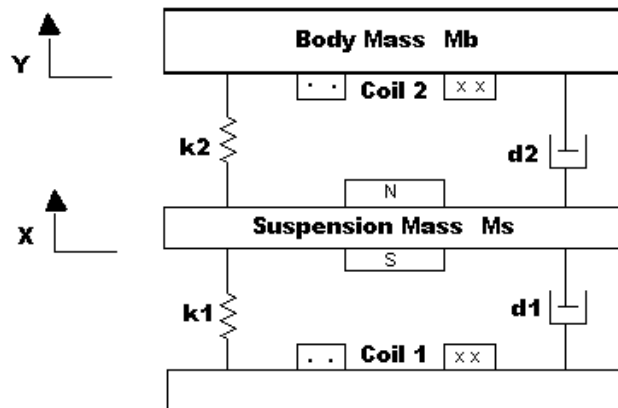


Figure 1.3: Mechanical Representation of New Suspension System

The suspension system includes among the common parameters two coils (coil-1 and coil-2) and permanent magnets. The excitation coil (coil-1) produces the road vibration while the damper coil (coil-2) produces the control force that will keep the vehicles body from moving. The coils are of copper material. The parameters of the suspension model and their values are:

$$M_b = \text{Vehicle body mass} = 1.8kg$$

$$M_s = \text{Vehicles suspension mass} = 1.6kg$$

$k_1 = \text{spring constant of wheel and tire} = 1600\text{N/m}$

$k_2 = \text{spring constant of suspension} = 1400\text{N/m}$

$d_1 = \text{damping constant of wheel and tire} = 10\text{Ns/m}$

$d_2 = \text{damping constant of suspension} = 15\text{Ns/m}$

$X = \text{displacement of suspension}$

$Y = \text{displacement of vehicle's body}$

The mass of the suspension and the vehicle's body were measured using a regular scale. To measure the spring constants an apparatus was used that graphed the masses that we attached to the spring versus the spring displacement. Since $F = kx = mg$, where k is the spring constant, x is the displacement and g is the gravitational constant, the ratio obtained is $\frac{k}{g} = \frac{m}{x}$. Therefore; the slope of the graph is multiplied with g to get the value of the spring constants. The values of the damping coefficients are chosen to achieve a minimal oscillation in the vehicles body. Different suspension systems have diverse damping coefficient which depend on the type of terrain the vehicle is used.

The unevenness of the road will give the wheel a vibration. This vibration will be represented as a force $F(t)$, that will disturb the equilibrium of the system. In our model the road conditions will be simulated and represented as a current signal which will be applied to coil-1. In the following the existence of $F(t)$ is assumed in the system to derive its counteractive forces. This will help to derive the differential equations necessary to represent this system as an electrical circuit. To facilitate the understanding of these derivations the free body diagrams were constructed for each of the masses with the corresponding forces that are acting upon them. These diagrams are shown in the Figure 1.4.

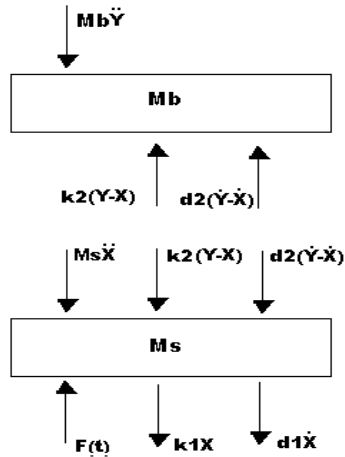


Figure 1.4: Free Body Diagrams of System

The forces acting on the suspension system shown above and their descriptions are listed in Table 1.1.

Table 1.1: Forces acting on Ms and Mb and their description

- Ms: $F(t)$ = force due to the unevenness of the road
 k_1X = force of the wheel spring = $k_1 * \text{displacement}$
 $d_1\dot{X}$ = force of the wheel damping = damping * velocity
 $M_s\ddot{X}$ = force of the suspension system = mass * acceleration
 $k_2(Y - X)$ = force of the suspension spring = $k_2 * \text{displacement}$
 $d_2(\dot{Y} - \dot{X})$ = force of the suspension damping = damping * velocity
- Mb: $k_2(Y - X)$ = force of the suspension spring
 $d_2(\dot{Y} - \dot{X})$ = force of the suspension damping
 $M_b\ddot{Y}$ = force of the mass of the vehicle body

The k_1 and k_2 represent the spring constants of the system. From the free body diagrams and the knowledge that to achieve equilibrium the sum of all forces must equal to zero, the equations of the motion of a suspension system are derived.

$$F(t) = M_s\ddot{X} + k_1X + d_1\dot{X} + k_2(Y - X) + d_2(\dot{Y} - \dot{X}) \quad (1)$$

$$M_b\ddot{Y} = k_2(Y - X) + d_2(\dot{Y} - \dot{X}) \quad (2)$$

Equations (1) and (2) are similar to the ones used to describe the sum of the voltages in an electrical circuit that consists of resistors, inductors and capacitors. The supply voltage of the circuit is the $F(t)$ force since it is the one responsible for the presence of the others. If the main currents of the system were represented as \dot{X} and \dot{Y} then the

electrical circuit will be a combination of resistors capacitors and inductors connected in series and parallel with each other. The voltage drop across a resistor is $V = I * R$ and since $I = \dot{X}$ or \dot{Y} then the damping coefficients will be resistors in the electrical circuit. The same knowledge was applied to the other variables of the equations. Knowing that the voltage drop of an inductor is $V = L \frac{dI}{dt}$ and of the capacitor is $V = \frac{1}{C} \int I$, the masses of the system were represented as inductors and the $\frac{1}{k}$ as capacitors where k is equal to the spring constant. Therefore from the equations above it was possible to derive an electrical circuit to demonstrate the movement of a vehicle suspension system. The equivalent electrical circuit schematic of the system is shown in Figure 1.5.

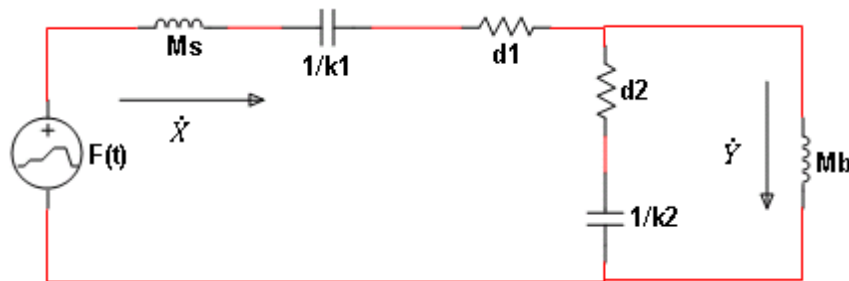


Figure 1.5: Electrical Representation of the Suspension System

This electrical circuit will help to derive a reliable control system that will achieve stability for the body of the vehicle regardless of road conditions. This means that modification will be done to the circuit so that the current \dot{Y} is minimal. The analysis and simulations of this circuit for different types of road conditions were done using the PSPICE program. The circuit above is converted into the appropriate Code 1 used by the program.

Code 1: PSPICE Code of the Electrical Circuit

```
Suspension System
Vroad 1 0 PULSE(0V 1V 1s 1us 1us 20s 40s)
Ck1 1 2 0.000714285714
Lms 2 3 1.6
Rd1 3 4 10
Lmb 4 0 1.8
Ck2 4 5 0.000862068966
Rd2 5 0 15
.PROBE
.TRAN 6 6 0 100m
.END
```

First the suspension system is given a step input for the $F(t)$. The input signal and the current that goes through the inductor M_b is show in Figure 1.6.

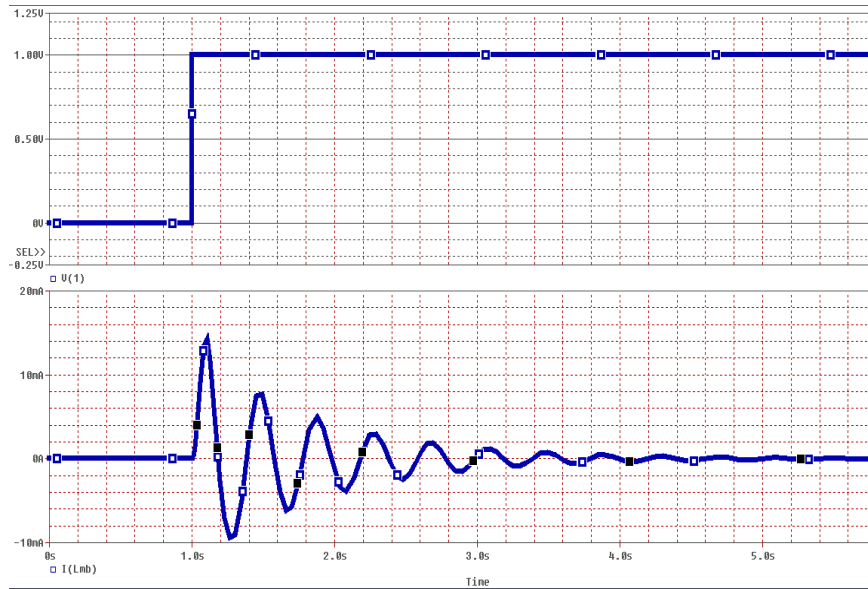


Figure 1.6: Step Input signal $F(t)$ and Current through Inductor M_b , Y

Figure 1.7 shows that the step input of the road ($F(t)$) will produce large vibrating velocity to the vehicles body (\dot{Y}). The \dot{Y} velocity will slow down and it will take up to 4 seconds for the vehicle’s body to stop moving which is a long time. Next is shown how the circuit reacts to an impulse signal. The $F(t)$ signal will represent a bump in the road and the results describe the response of the suspension system. The code in this case will remain the same except for the input voltage which is written in Code 2:

Code 2: Impulse Signal Representing a Bump in the Road

```
Vroad 1 0 PULSE(0V 1V 1s 1us 1us 0.5s 40s)
```

The response of the system due to this input is shown in Figure 1.7.

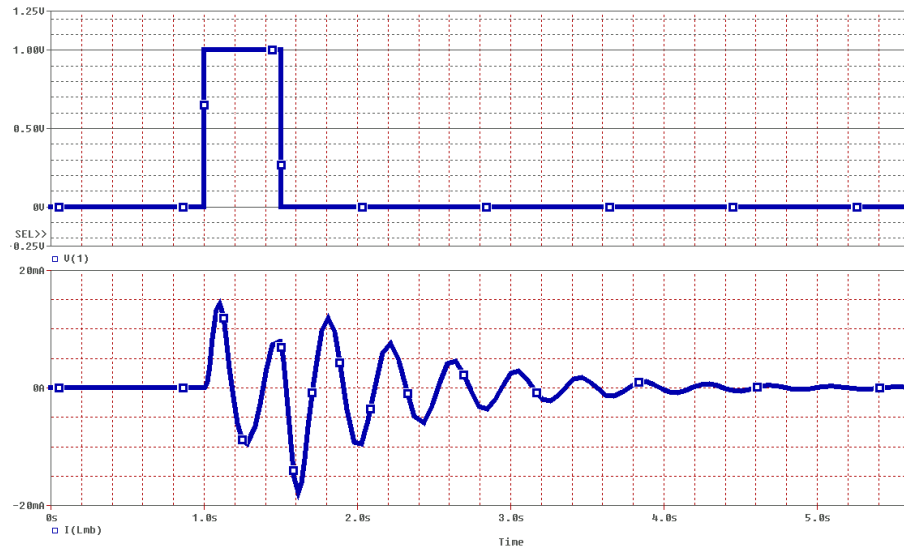


Figure 1.7: Impulse Input Signal V(1) [F(t)] and Current through Inductor Mb I(Lmb) [Y]

The figure shows that the system will have a greater vibration in the beginning but the time of recovery will be slightly different.

An important parameter to calculate is the resonance frequency of the system. In this frequency the suspension system oscillates at its maximum amplitude. This frequency is used to coordinate the control system to give a signal that will revolve around this value. To find this frequency an AC analysis of the circuit is done using PSPICE. To determine the resonance frequency, the system is fed with a sinusoidal sweep voltage that ranges from the smallest to the highest possible frequency that the system is expected to operate on. The Code 3 for this type of analysis is shown.

Code 3: Frequency Analysis of the Suspension System

```
Suspension System
Vroad 1 0 AC 1
Ck1 1 2 0.000714285714
Lms 2 3 1.6
Rd1 3 4 10
Lmb 4 0 1.8
Ck2 4 5 0.000862068966
Rd2 5 0 15
.AC OCT 1000 0.0001 15
.PROBE
.END
```

The current that flows through inductor Mb vs. frequency is shown in the Figure 1.8.

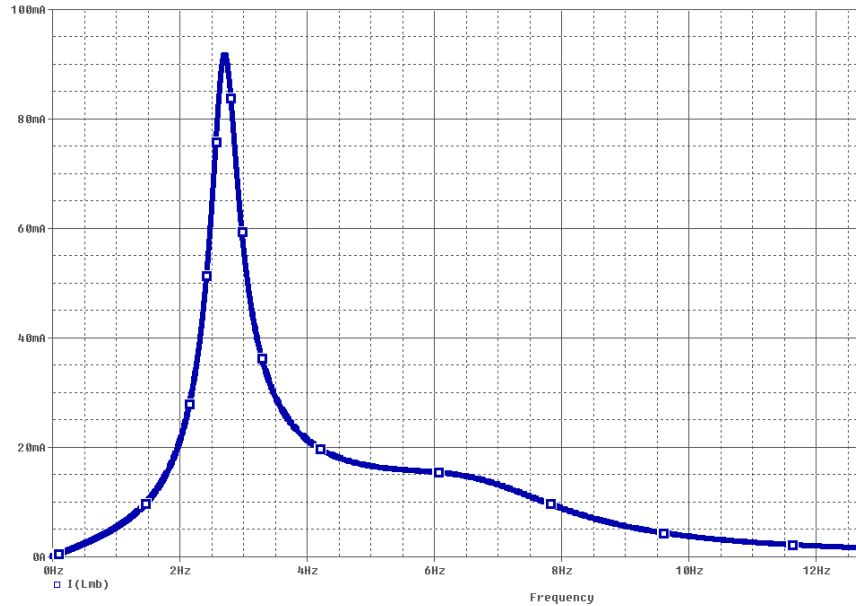


Figure 1.8: Current through Mb with Respect to Frequency

The graph above shows in distinction the value of the resonance frequency when the body of the vehicle achieves maximum oscillation. The system will resonate at around 2.7Hz and at this frequency the velocity of the vehicle's oscillations can grow up to 0.1m/s with a force of just 1N peak produced by the road.

The results of this section are necessary in the development of the control system used to eliminate the vibrations of the vehicles body. The electrical circuit derived will be used in the following sections as a reference for the different types of circuitry needed to achieve this goal.

2. System Design: Block Diagram

After analyzing the system an overall block diagram was designed to have a general view of the signal flow of the shock absorber system. This signal path was designed based on the mechanical system previously shown. The overall block diagram of the system design is shown in Figure 2.1. Specific parameter for each of the modules will be provided in a later section.

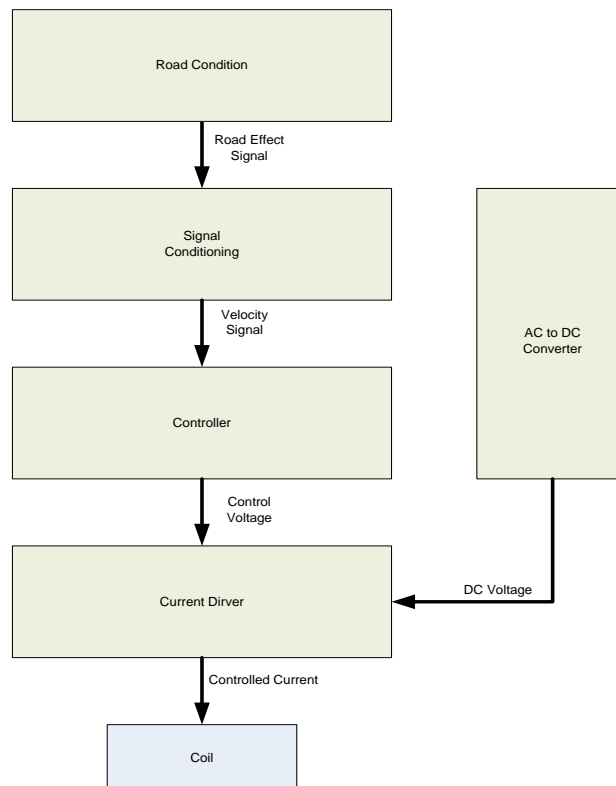


Figure 2.1: Overall Block Diagram

The road condition module generates a force similar to the effects of a bumpy road. The signal condition module records the movement provided by the road condition module and provides a modified output signal. This output is processed by the controller to achieve the necessary control signal. The current driver uses this signal to control the current flowing through the coil. The controlled current flowing through the coil will then cause the necessary effects to oppose the force produced by the road condition module. As a result, the body of the vehicle will not have any vertical movement regardless of road conditions. The AC-to-DC converter module is used to supply the necessary power to the system.

3. Road Condition Module

Different road conditions simulations are needed to help construct a control circuit for the suspension system. The road system has to produce a variety of forces at different frequencies. The road conditions module will be connected to the excitation coil (coil-1) of the lower block. The module will create a signal similar to the effect of the road on the suspension system and will be controlled by a current source flowing through the excitation coil. A magnetic field is created around the suspension mass, M_s , due to the interaction between the magnet and the electric field generated at the excitation coil when current flows through it. When those fields enter into contact, they attract each other if the polarities are opposite and repel if the polarities are equal moving the model accordingly. A DC voltage supply is used to supply this circuit and the coil with the necessary current and voltage. Figure 3.1 shows a generic representation of this system.

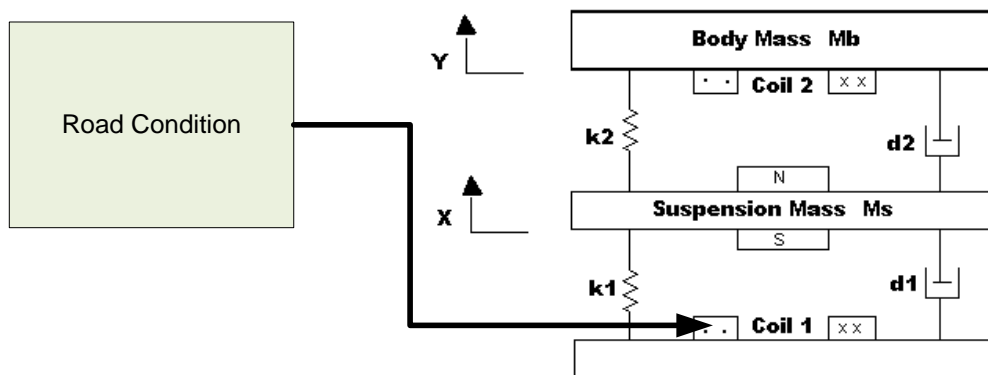


Figure 3.1: Road Condition and Its Corresponding Connections

3.1 Prior Art Research

After an extensive research, many useful way and techniques were encountered to implement the Road Condition module. A function generator or oscillator is necessary to generate the varying signal. This circuit will produce a variable sine, triangular or rectangular signal to represent the different road conditions. The current flowing through the excitation coil can be controlled by connecting a transistor in series with it. The transistor can then be driven by the output signal of the oscillator which can be manually or automatically adjusted.

3.1.1 Oscillator

Different types of oscillators were taken into consideration for our system. First the rectangular oscillator was tested. This oscillator did not work properly for this application due to the fact that during the high or low states, the step response remained constant for a period of time. This caused a large amount of current flowing through the coil consequently sinking most of the voltage supplied by the DC power supply.

Many methods and ICs were found that generated a sine wave such as a digitally controlled sine wave generator. It was able to produce an accurate sine wave with an adjustable frequency. This generator however, required different IC components to produce the desired output which were expensive and not simple to implement. The system schematic required to produce the sine wave generator is shown in Figure 3.2.

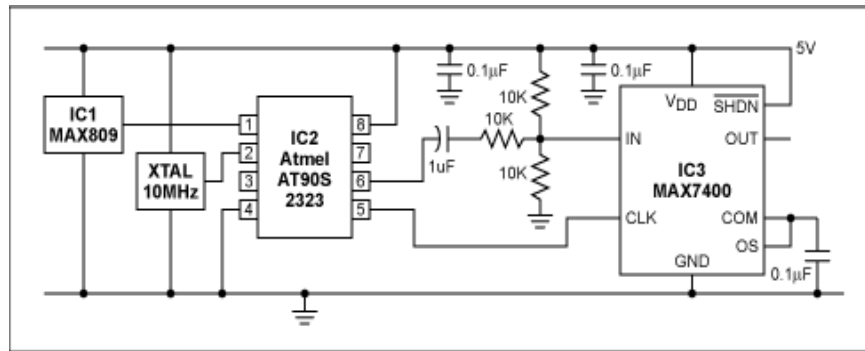


Figure 3.2: Digital Controlled Sine Wave Generator (3)

After a more carefully analysis of the system it was concluded that a triangular wave was more suitable to implement as part of the road condition module. Continuing with the research, many techniques were found to generate triangular waves. One triangular wave generator technique in particular called the attention. It only uses two op-amps, one capacitor and a few resistors. This means it will be inexpensive and very simple to implement. From the generic schematic shown in Figure 3.3 it is clear that this particular wave generator seems to be appropriate for the system.

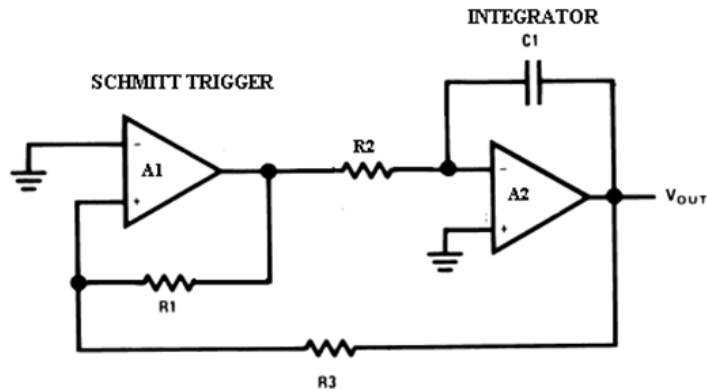


Figure 3.3: Generic Triangular Wave Generator

This triangular wave generator can be implemented with two main circuit blocks. One is an integrator circuit which is composed of one op-amp, one capacitor and one resistor with a negative feedback configuration. The second circuit block is a comparator or similarly known as a Schmitt Trigger which is composed of one op-amp and one resistor configured in a positive feedback. The result of combining those two circuit blocks gives a triangular and a square wave. The triangular wave is the output of the integrator circuit block and the rectangular wave is the output of the Schmitt Trigger circuit block.

The configuration of the Schmitt Trigger consists of an op-amp and a resistive voltage divider connected in a positive feedback path. The negative input of the op-amp is connected to ground. When an op-amp is connected for positive feedback, its output can be either high (positive) or low (negative) if there is a slight change in V_{in} . When the op-amp is connected to the voltage supplies $+V_{SS}$ and $-V_{SS}$, only two stable states are expected from this op-amp configuration. When the input voltage exceeds few positive mV the output voltage becomes positive. When the input falls below a few negative mV the output voltage becomes negative. The Schmitt trigger and its output are shown in Figure 3.4 .

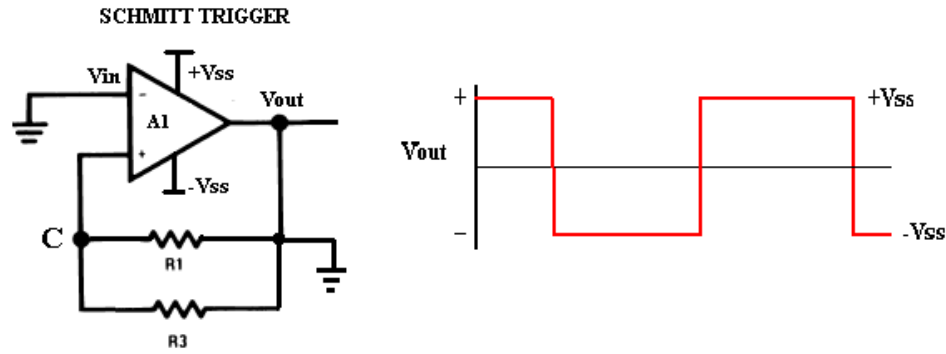


Figure 3.4: Schmitt Trigger Circuit and its Output

The configuration of the integrator consists of an op-amp connected with a capacitor in a negative feedback loop. The signal is entered into the negative input of the op-amp which is connected to a resistor. The positive input of the op-amp is connected to ground. When an op-amp is connected in a negative feedback with a capacitor the output signal is the integral of the input one. This occurs because the capacitor current and voltage change with respect to time. This means that if we add a constant positive voltage to the input, we expect to see a ramp with positive slope as time changes at the output. An example of the integrator operation is shown in Figure 3.5 when a square signal is applied to its negative input while the positive input is connected to ground.

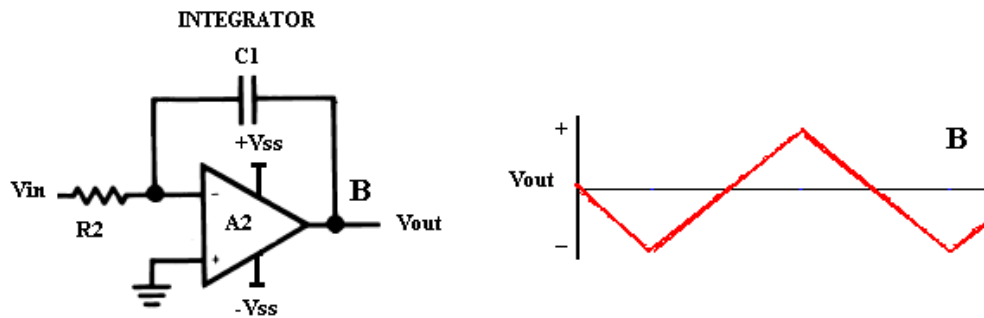


Figure 3.5: Integrator circuit and its output

The combination of these two circuits gives an overall operation that is ideal for application in the system. The expected behavior of this oscillator and its diagram are shown in Figure 3.6.

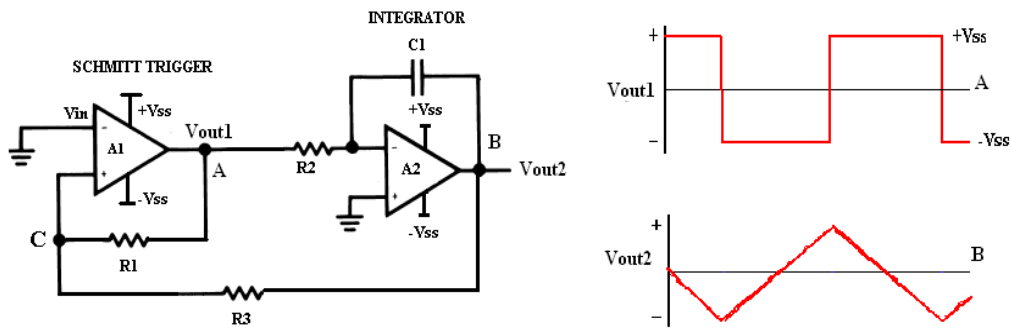


Figure 3.6: Triangular Wave Generator and its Outputs

3.1.2 Controlled Voltage Source

After careful analysis it was concluded that a transistor is able to control the current needed to drive the excitation coil. A Bipolar Junction Transistor (BJT) will be able to drive this current efficiently. The design of the road condition module is described in the following section.

3.2 Road Condition Block Diagram

Using the information gathered from the previous section the block diagram of our Road Condition module is shown in Figure 3.7.

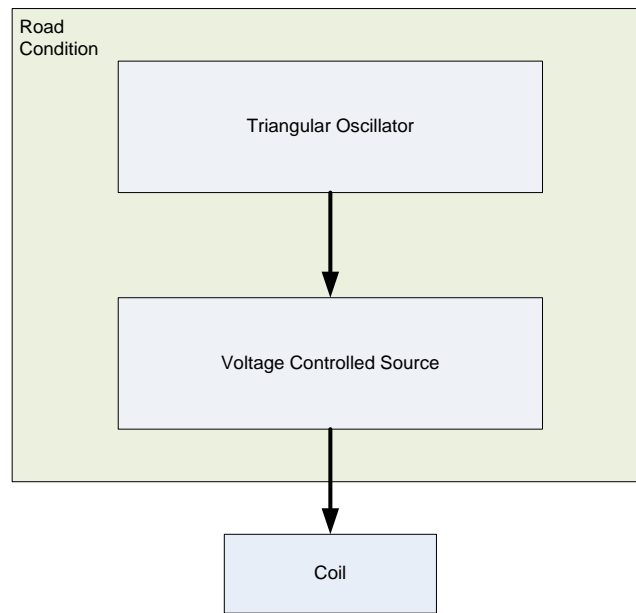


Figure 3.7: Road Condition Block Diagram

Using this diagram and the information gathered we constructed our module to simulate the road conditions in our model. In the following we will describe the design and construction of each of the sub-modules.

3.2.1 Oscillator Design

As we discussed in the previous sections a triangular wave generator is going to be used to represent the road conditions of the system. To achieve this it was concluded a circuit that consists of a Schmitt trigger and an integrator needed to be constructed. From the previous analysis the resonance frequency of the system was found to be around 2.7 Hz. Therefore the frequency range of the signals should include this value. Also the output signal was chosen to have maximum amplitude of 10V to limit the number of power supplies. The circuit of the triangular wave generator is shown in the Figure 3.8.

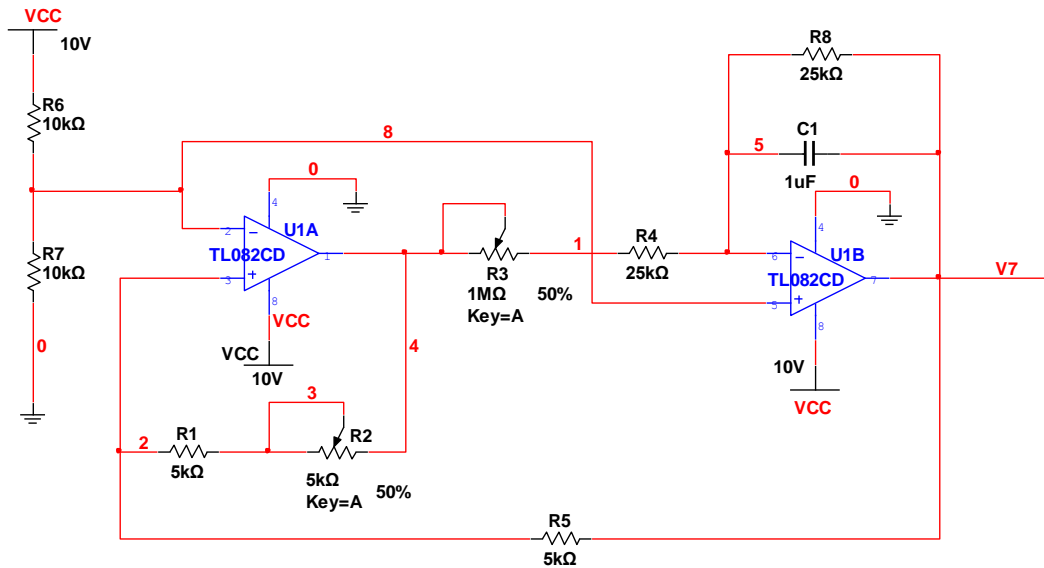


Figure 3.8: Final Triangular Wave Generator Schematic

The components of the circuit are supplied by a 10V DC source labeled V_{CC} . The negative rails of the op-amps are connected to ground to limit the number of voltage supplies to one. Due to this change a 5V DC reference voltage was added to the negative input of the Schmitt Trigger and to the positive input of the integrator to represent virtual

ground. This means that the oscillations will be riding at a 5V DC. The resistors R₅ and R₇ are used as a voltage divider to achieve this desired voltage from the 10V DC source.

Two potentiometers were added to control the amplitude and frequency of the output signal. Potentiometer R₂ in series with the resistor R₁ will achieve variety in the amplitude of the oscillations. The maximum value of R₂ was chosen to be 5kΩ to limit the maximum frequency range of the output signal to 20 Hz. In order for the circuit to generate oscillations, the condition (R₁ + R₂) ≥ R₅ ≥ 1 is required by the frequency equation shown in Equation (3). This means that when potentiometer R₂ is off, the minimum value of (R₁ + R₂) = 5kΩ therefore meeting the required condition (R₁ + R₂) ≥ R₅ ≥ 1 to generate oscillations.

$$f = \frac{1}{4 \cdot C_1 \cdot (R_3 + R_4)} * \frac{R_1 + R_2}{R_5} \quad (3)$$

Potentiometer R₃ was added in series with the resistor R₄ to vary the frequency of the signal. The maximum value of R₃ is chosen to be 1MΩ to limit the minimum frequency range of the output signal to 0.244 Hz. The same reasoning was used to determine the values of R₁ and R₄. The capacitor C₁ was chosen 1μF to allow the circuit to work in low frequencies. Calculations of these frequencies using the frequency equation are shown below.

When the potentiometer R₂ = 5KΩ:

$$f_{\min} = \frac{1}{4 \cdot (1 \mu F) \cdot (1 M\Omega + 25 K\Omega)} \cdot \frac{(5 K\Omega + 5 K\Omega)}{5 K\Omega} = 0.487 Hz$$

$$f_{\max} = \frac{1}{4 \cdot (1 \mu F) \cdot (0 \Omega + 25 K\Omega)} \cdot \frac{(5 K\Omega + 5 K\Omega)}{5 K\Omega} = 20 Hz$$

When the potentiometer R₂ = 0Ω:

$$f_{\min} = \frac{1}{4 \cdot (1 \mu F) \cdot (1 M\Omega + 25 K\Omega)} \cdot \frac{(5 K\Omega + 0\Omega)}{5 K\Omega} = 0.244 Hz$$

$$f_{\max} = \frac{1}{4 \cdot (1 \mu F) \cdot (0 \Omega + 25 K\Omega)} \cdot \frac{(5 K\Omega + 0\Omega)}{5 K\Omega} = 10 Hz$$

Simulation Results

The results above were used to simulate the triangular wave oscillator. To verify the proper operation of this circuit both potentiometers were set to their maximum values and simulated for about 500mS. The signal at the outputs of the Schmitt Trigger and integrator are shown in Figure 3.9.

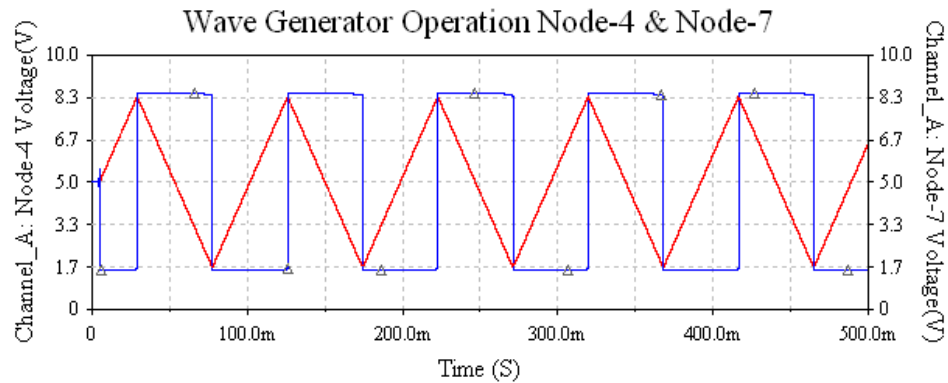


Figure 3.9: Wave Generator Simulation Outputs of Node-4 & Node-V7

The figure shows that the desired voltage was achieved. Once the proper operation of the circuit was proved, its maximum and minimum frequencies were tested when $R_2 = 5K\Omega$. This time only the output signal of the circuit was observed. The results obtained are shown in Figure 3.10. The simulations showed that $f_{min} \cong 0.4 Hz$ and $f_{max} \cong 20 Hz$ which are the same frequencies estimated by the frequency equation.

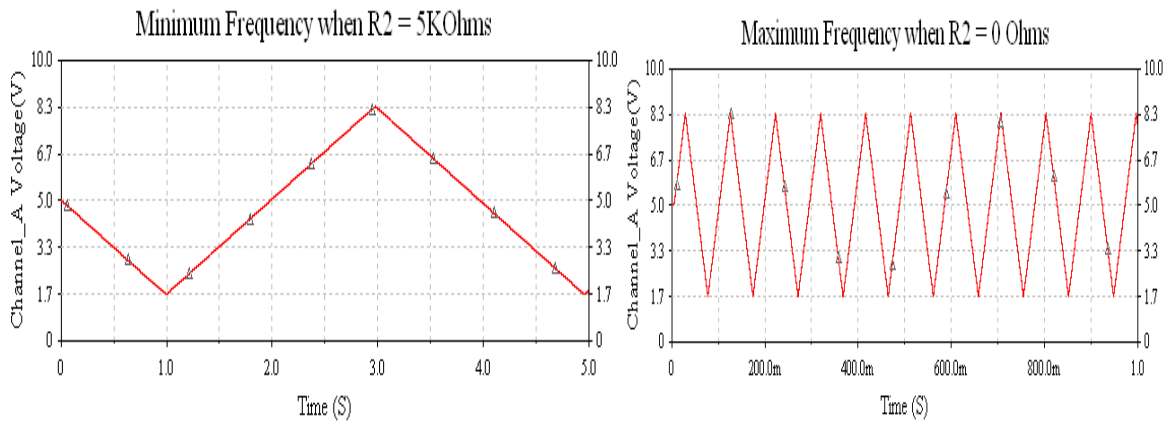


Figure 3.10: Min Frequency when R2 = 5K Ω and Max Frequency when R2 = 0 Ω

Next the circuit was tested for varying amplitude. This time potentiometer R_2 was adjusted. The results are shown in Figure 3.11. The simulations showed that as R_2 was adjusted, the amplitude of the output signal changed with respect to time.

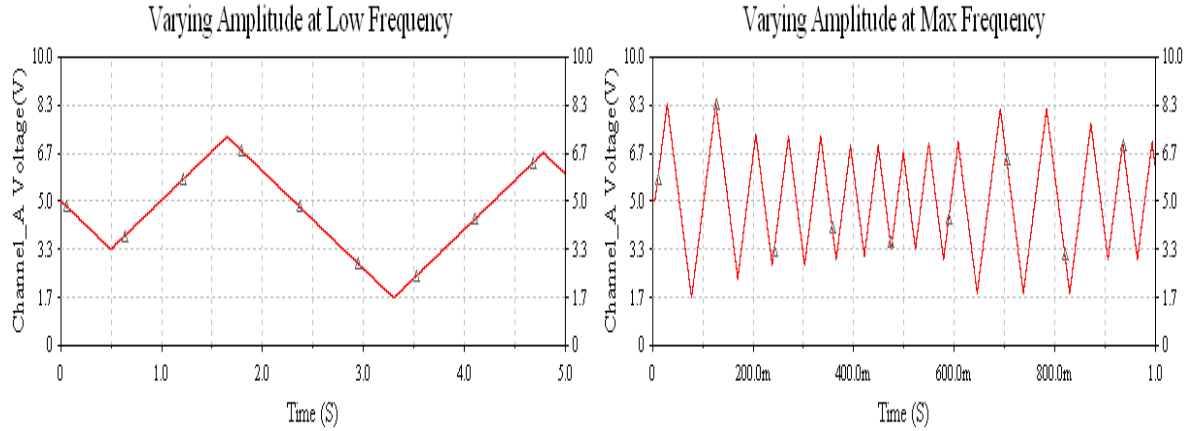
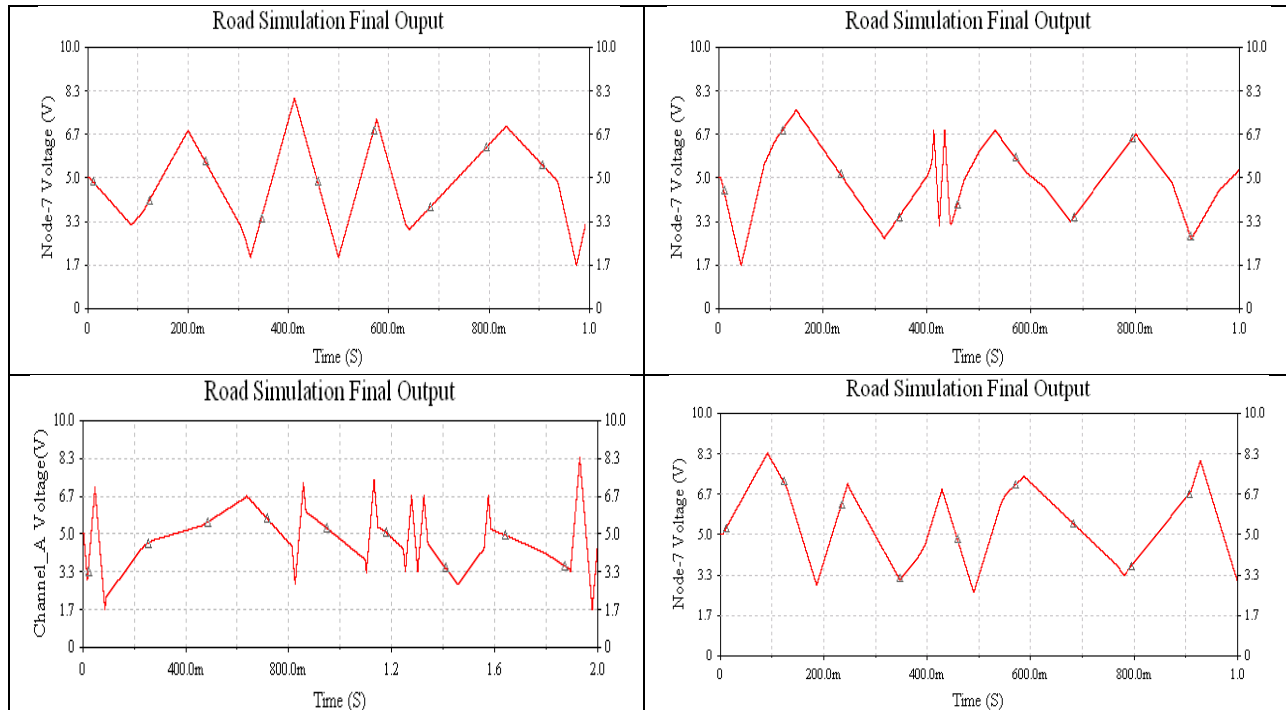


Figure 3.11; Varying Amplitude at Min & Max Frequency

The results of the simulations also show that the circuit will perform efficiently and give the adequate signal to be used by the current controller. Examples of different output signals due to randomly adjusting the two potentiometers are shown in Table 3.1.

Table 3.1: Varying Amplitude at Different Frequencies



Prototype

Research for the components needed to build the circuit was done after the desired behavior was obtained from the simulation results. These components were located through the use of websites like Dig-key and Mouser. The TL082 op-amp is shown in Figure 3.12.

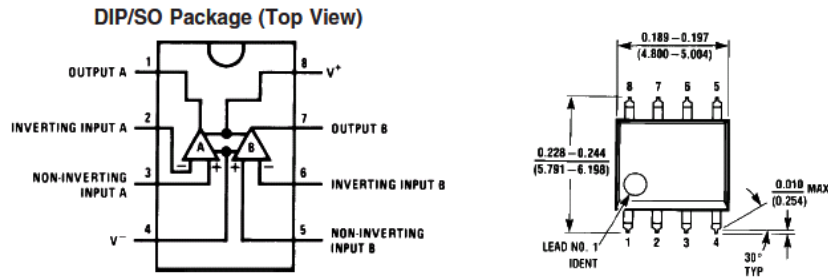


Figure 3.12: TL082 op-amp (4)

The behavior of the output voltage with respect to different loads and the bode plot diagram of this component are shown in the Figure 3.13.

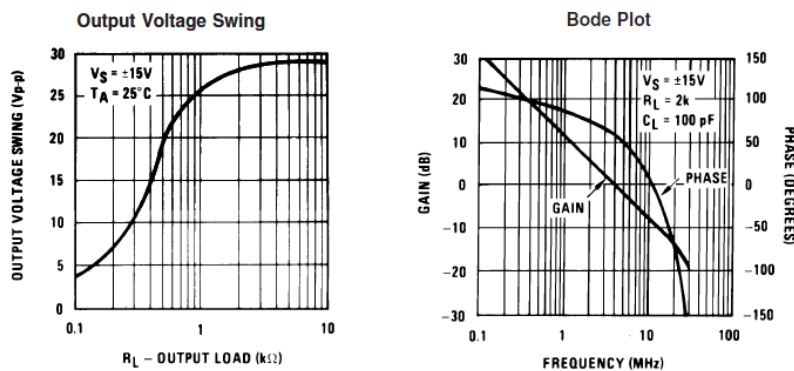


Figure 3.13: Characteristics of TL082 op-amp (4)

The $5\text{K}\Omega$ (53C15K) and $1\text{M}\Omega$ (381N1MEG) potentiometers that we needed for the circuit are shown in Figure 3.14. The complete oscillator circuit including all its components is also shown in Figure 3.14.

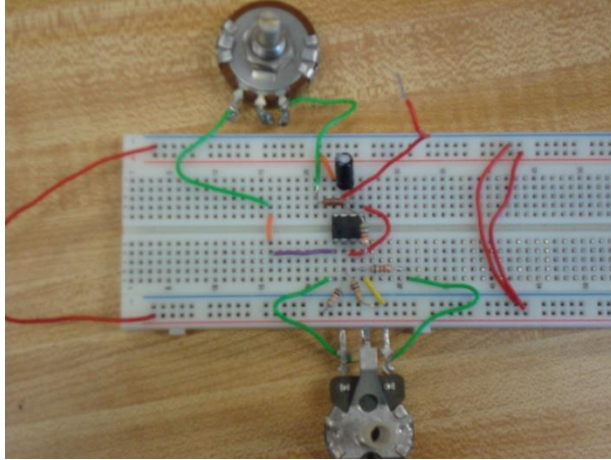


Figure 3.14: Triangular Wave Generator Circuit

After the circuit was built, it was tested extensively for various real road scenarios. To do this, the potentiometers were manually adjusted to a random value to test the reliability and efficiency of the circuit. The results were positive and some of these are shown in the following figures. Figure 3.15 shows the maximum and minimum frequencies produced by the circuit. Figure 3.16 shows the results when the potentiometers are adjusted to a random value.

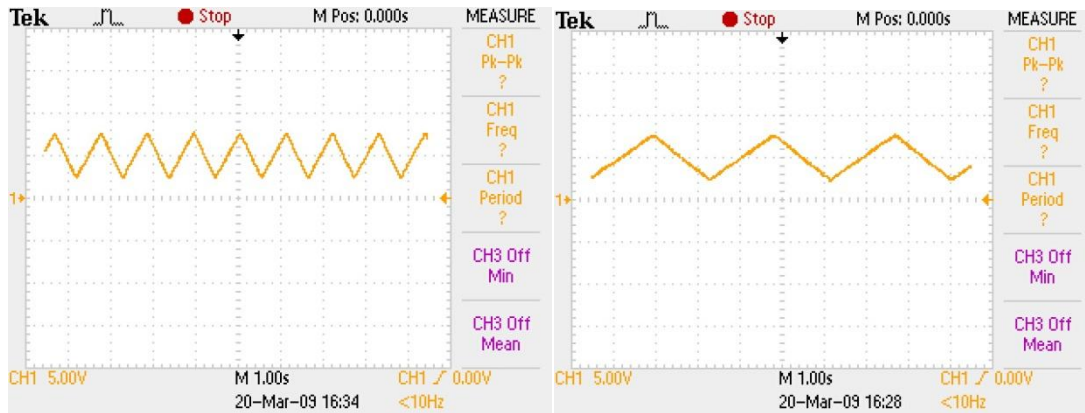


Figure 3.15: Oscillator at Maximum and Minimum Frequency

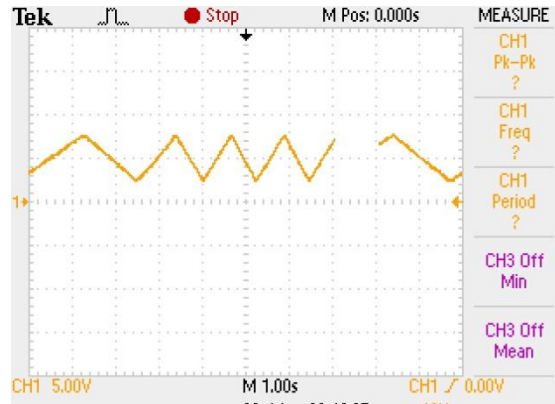


Figure 3.16: Oscillator at a Random Frequency

3.2.2 Voltage Controlled Source Design

The signal from the triangular oscillator is used to drive our voltage controlled source. The design for this module consisted of a BJT that is able to handle the current flowing through coil-1. A Darlington connection was used due to the magnitude of the current. The connection of this circuit is shown in the Figure 3.17.

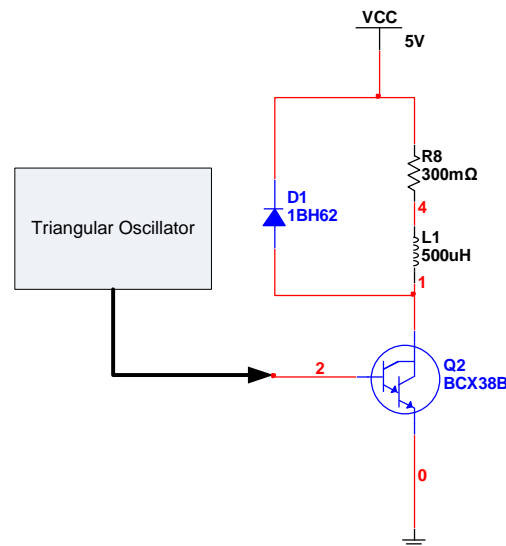


Figure 3.17: Voltage Controlled Schematic and Its Corresponding Connections

The figure shows that the signal from the triangular oscillator is connected to the base of the Darlington. The collector is connected to coil-1 which is supplied with the necessary signal by a DC voltage supply. A diode is connected in parallel with the coil for

protection and safety precaution. The excitation coil internal resistance is labeled R_8 which was measured to be close to $300\text{m}\Omega$ and its inductance is labeled L_1 . The value of L_1 was calculated by connecting a resistor in series with the coil and a function generator. Figure 3.18 shows this connection.

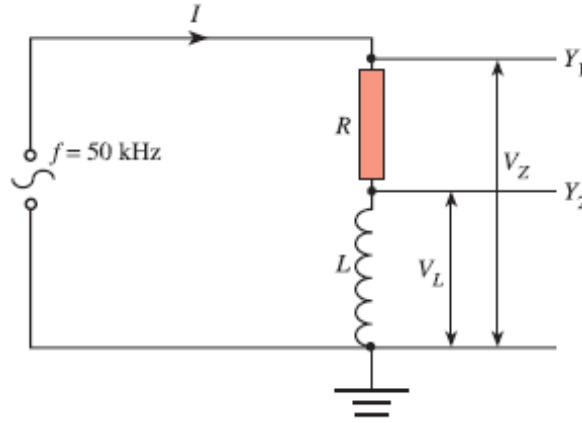


Figure 3.18: Comparison of voltages V_Z and V_L (6)

The circuit is supplied with a sinusoidal wave. To simplify the calculation, ω ($2\pi f$) and R are chosen such that $R \gg \omega L \gg r$ or $\omega L \gg R \gg r$. This is accomplished by choosing $R = 24\text{k}\Omega$ and $f = 50\text{ kHz}$. An oscilloscope is used to measure the peak-to-peak voltage across Z (V_Z) and R (V_R). Since $V_L = I * X_L$ equation (4) is derived. (6)

$$V_L = \frac{V_Z}{Z} \omega L = \frac{V_Z \omega L}{\sqrt{R^2 + (\omega L)^2}} \approx \frac{V_Z}{R} \omega L \quad (4)$$

The value for ω was calculated to be about $314\text{E}+3$ rads/sec as it shown in the following calculation.

$$\omega = 2 * \pi * f \cong 314 * 10^3$$

The results from the oscilloscope readings are: $V_L = 0.26\text{ V}$ and $V_Z = 38\text{ V}$. This gave all the information needed to calculate the inductance of the excitation coil. The value obtained after the calculation was performed was about $523\mu\text{H}$. For simplicity, the value $L_1 = 0.5\text{mH}$ was chosen to be used in the simulations.

$$L = \frac{V_L R}{V_Z \omega} \cong 0.523\text{ mH}$$

The voltage drop across the transistor changes if the current applied to its base changes. This causes a change in the current flowing through the inductor L_1 which varies its electric field. As a result, the magnitudes of the oscillations on the suspension system also change.

Simulation Results

The circuit was simulated using the MULTISIM program to analyze its output signals. The Darlington was supplied with a 5V DC voltage source for simulation purposes. The results obtained are shown on Figure 3.19.

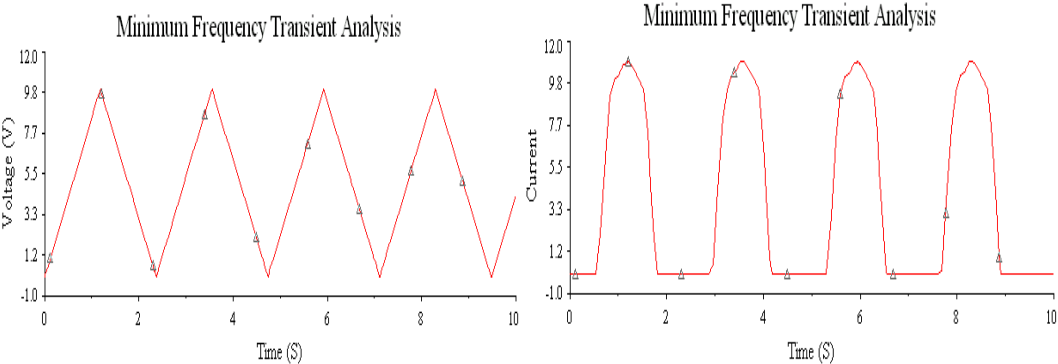


Figure 3.19: Input and Output Signals of the Voltage Controlled Source at Minimum Frequency

The simulation results showed that when the transistor was driven by a triangular wave at a frequency of about 0.4Hz the current in the coil ranges from about 0A to about 10A at the same frequency. This changing current will then generate the required electrical field to create the effect of a bumpy road on the wheel. When the transistor experiences a triangular wave at a frequency of about 20Hz the current in the coil also ranges from about 0A to about 10A at the same frequency as it shown in Figure 3.20.

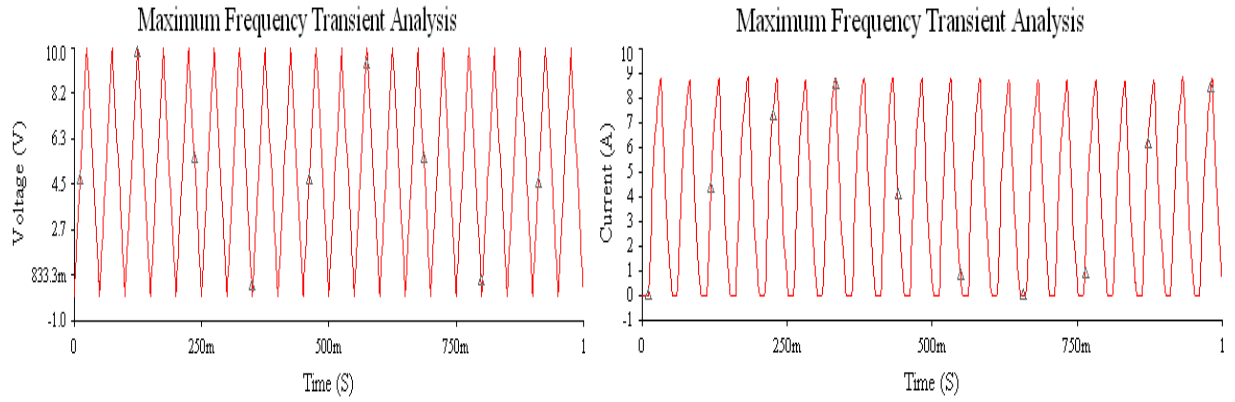


Figure 3.20: Input and Output Signals of the Voltage Control Source at Maximum Frequency

Prototyping

The components needed to build the designed circuit were researched after the desired behavior was obtained from the simulation results. The inductor labeled L_1 for the circuit was the excitation coil from the mechanical system. The Darlington transistor used for this circuit is the QM50DY-2H and the type of diode used is the 1BH62. Figure 3.21 and Figure 3.22 below show the transistor and its characteristics respectively.

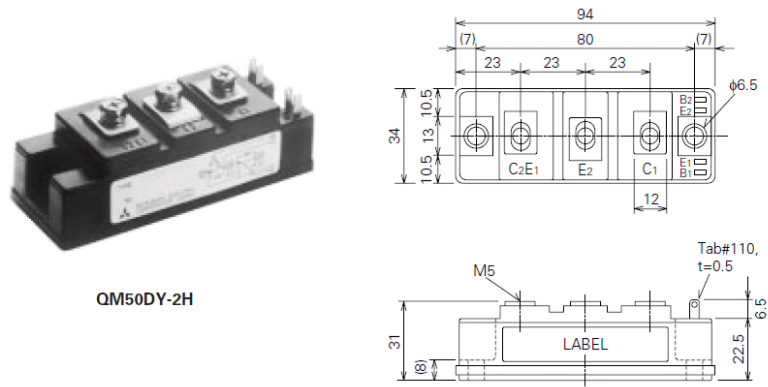


Figure 3.21: QM50DY-2H transistor (6)

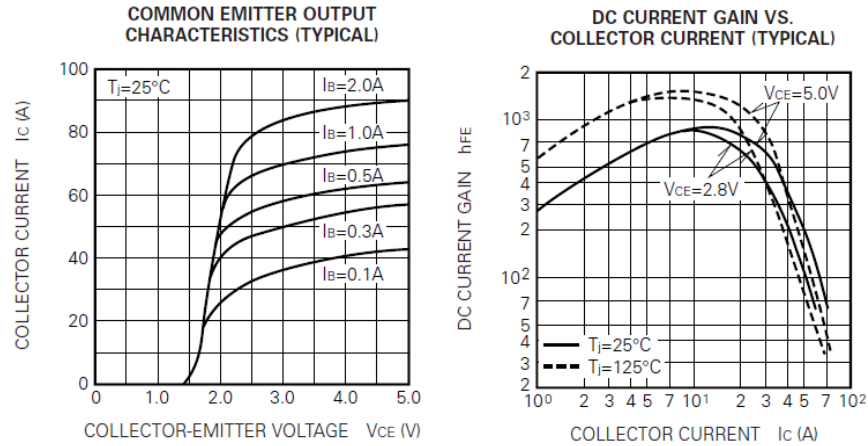


Figure 3.22: Characteristics of the transistor (6)

The circuit built for the voltage controlled source is shown in Figure 3.23. Only one of the diodes is used in a parallel connection with the transistor. The figure also shows the heat sinks used to keep the transistors and diodes from overheating. The complete circuit of the road condition module is shown in the appendix A.

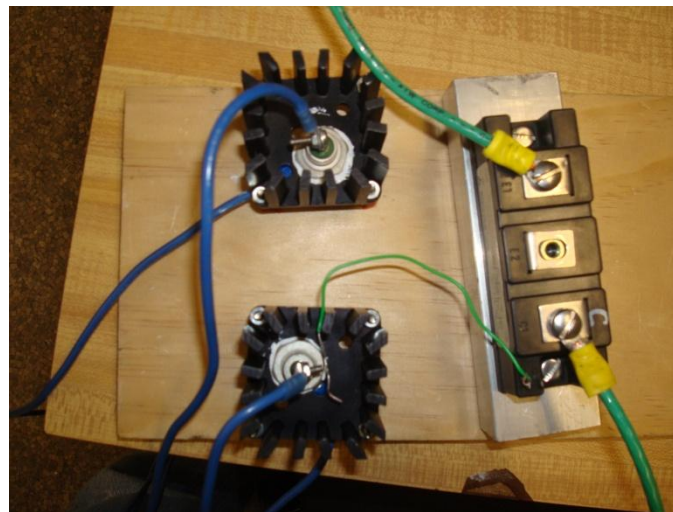


Figure 3.23: Voltage Control Source Circuit

The results acquired from the circuit built were similar to the ones produced by the simulations. A major difference was the amount of current that the coil and the BJT drew from the power supply. Simulations showed that the circuit needed up to 10A of current to operate. In reality the circuit drew around 20A which is twice as much as the predicted current from the power supply. The voltage needed to drive this current fluctuated between 15V to 3V.

4. Signal Conditioning

The signal condition module will record and modify the movements of the vehicle's body produced by the road condition module. Its objective is to read these vibrations caused by the bumpy road and transform them into a signal. The detailed block diagram of this module is shown in Figure 4.1.

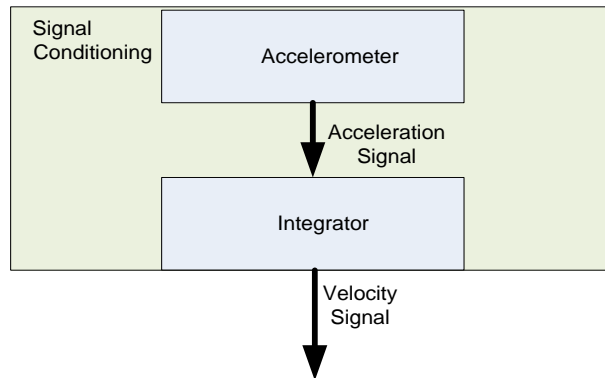


Figure 4.1: Block Diagram of the Signal Conditioning Module

The figure shows that an accelerometer and an integrator are used in this module. The accelerometer will provide with the acceleration signal of vehicle's body while the integrator circuit will produce its velocity. These sub-modules are described in details in the following sections.

4.1. Accelerometer

After some accurate research, the DE-ACCM3D accelerometer was used to measure the time variant acceleration of the model. Figure 4.2 shows the accelerometer and its dimensions.

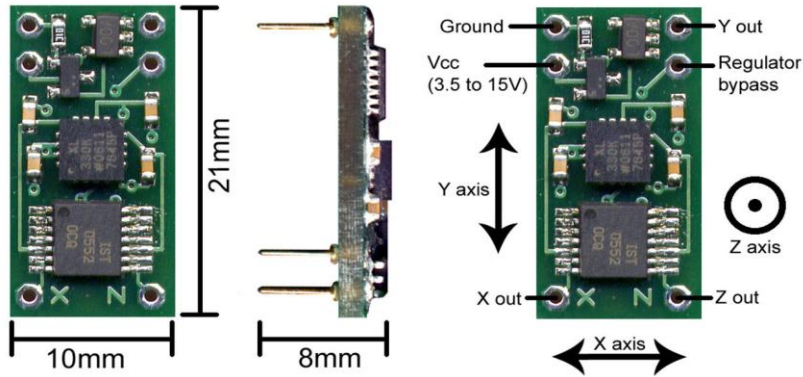


Figure 4.2: Accelerometer (7)

The DE-ACCM3D's features include:

- Ability to measure up to $\pm \frac{360mV}{g}$ ($g = \text{gravitational acceleration} = 9.81 \frac{m}{s^2}$)
- A wide range operating voltage (3.5 to 15V with an onboard regulator)
- Reverse voltage protection
- Output short protection
- integrated power supply decoupling
- Triple axis measurement

The accelerometer also allows the control of its sensitivity by varying the supply voltage provided to power it. Table 4.1 shows the typical sensitivities at deferent operating voltages

Table 4.1: Sensitivity of Accelerometer for each Operating Voltage

Operating Voltage	Sensitivity
3.6V	360 mV/g
3.33V (Default when using onboard regulator)	333 mV/g
3.0V	300 mV/g
2.0V	195 mV/g

Any operating voltage above 3.6 V will produce a sensitivity of 360 mV/g. Since the sensitivity of the device varies significantly with the supply voltage, a voltage regulator is

needed to keep the supply voltage constant and hence eliminate variations in the sensitivity of the accelerometer.

The onboard regulator of the accelerometer was used in this case to reduce the number of the components needed. A bypass capacitor of about 100pF was connected to the output of the regulator pin as directed by the manufacturer of the accelerometer. The regulator was supplied with 5V DC by choice since the sensitivity will remain 360mV/g. This will give the output signal of the accelerometer a virtual ground at 2.5V DC.

The accelerometer has three output ports that measure the acceleration depending on the way it is tilted. Since for this application there are only vertical movements, the X and Y outputs are left open and only the Z output is used. The output signal of the accelerometer is the acceleration of the model. This signal is then supplied to an integrator for modifications. Figure 4.3 shows this output signal.

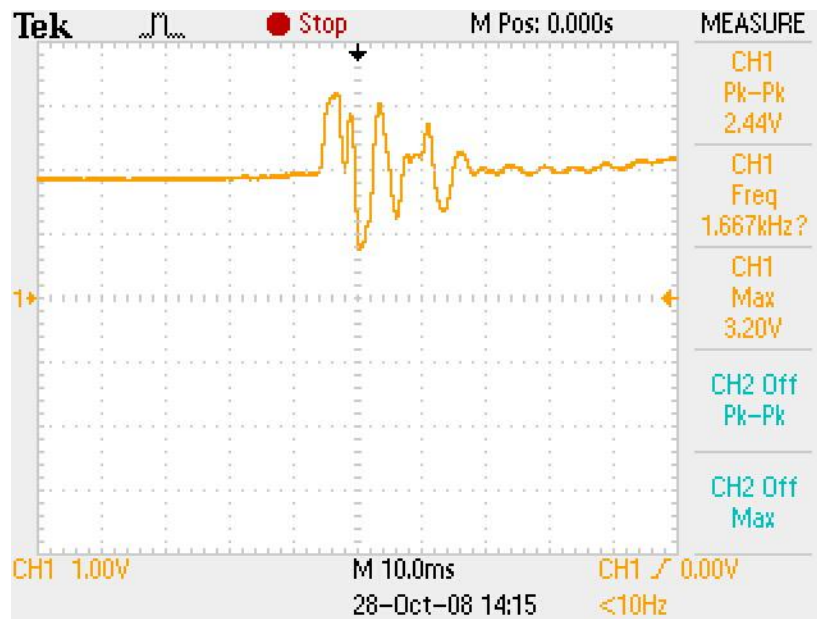


Figure 4.3: Accelerator Output Signal

The accelerometer is powered up by a 4V DC for proper operation. The accelerometer is quaked vertically and the Z output is connected to the oscillator to show the output signal in Figure 4.3. The output signal of the accelerometer is the acceleration of the model. This signal is then fed to an integrator circuit for desired modifications as it is explained in the following section.

4.2. Integrator

After obtaining a voltage signal that represents the acceleration of the vehicle's body modifications to this signal are done to obtain the velocity of the system. Using the knowledge that velocity is the integral of acceleration, an integrator circuit is needed to find the time variant velocity of the suspension system. Equation (5) shows the calculation that will be represented by this circuit.

$$v(t) = A \int a(t)dt \quad (5)$$

The integrator circuit will be similar to the one used in the oscillator for the road condition module. An analog approach for implementing this circuit was chosen because it was cheap and easy to implement. Figure 4.4 shows the schematic diagram of the integrator that was built.

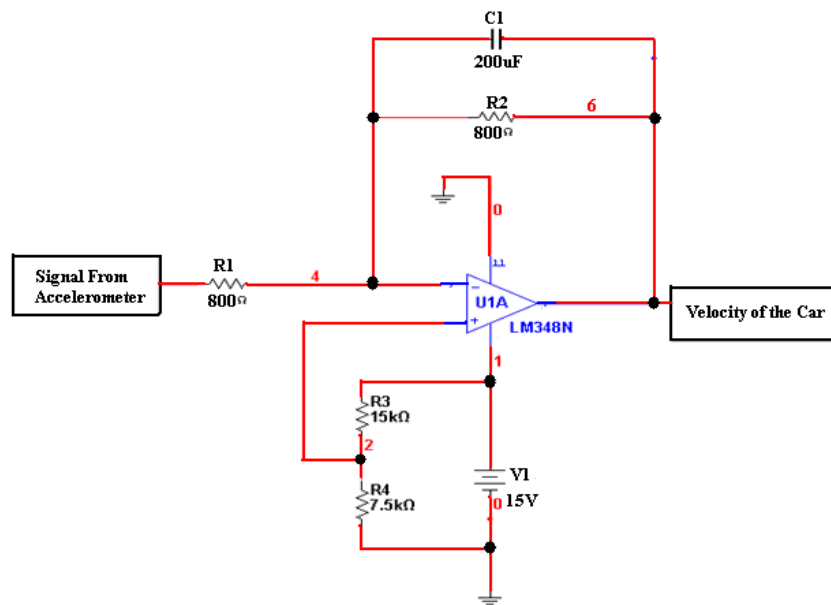


Figure 4.4: Integrator Circuit

The LM348N op-amp rails were powered with a 15V DC voltage and ground to eliminate the need of using two independent voltage supplies. Since the output signal of the accelerator has a DC offset of 2.5V the output of the integrator will always be at its maximum peak. In the beginning a coupling capacitor was added at the input of the integrator to block the DC offset. A large capacitor is needed because the signal that is

integrated runs at very low frequencies. However using large capacitors was very unpractical and inefficient. Therefore a decision was made to subtract out the DC offset instead.

The voltage divider at the non inverting input of the op-amp will not only subtract out the DC offset but also bring the DC level of the output down to 7.501V which is approximately halfway of V_{CC} . This produces a wider range of voltages for the input to swing without hitting the rails on the output. An important observation was that the integrator requires that the DC level of the input signal remains constant or it will give the wrong output signal.

The AC analysis of the integrator was performed to help find out how it performs over the appropriate frequency range. The frequency range that the integrator should perform is more or less between 0.2Hz to 20Hz. However it was almost impossible to design an integrator that would work properly in that frequency range. Therefore the specifications of the integrator were modified so it worked properly between 0.8Hz and 10Hz. The problem with the integrator designed was that its gain fell very fast with increasing frequency. As a result the output of the integrator at the maximum frequency is greatly diminished. Figure 4.5 and Figure 4.6 shows the frequency response of the integrator.

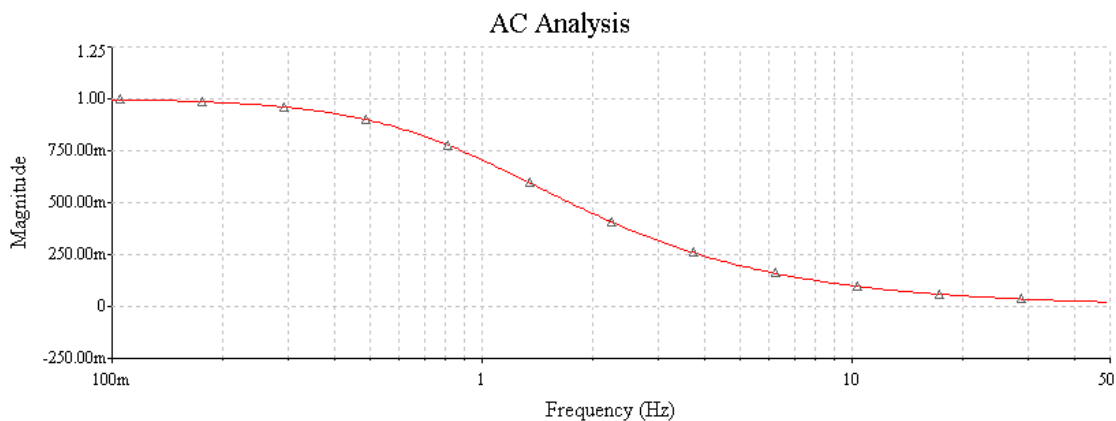


Figure 4.5: Magnitude Plot of the Frequency Response

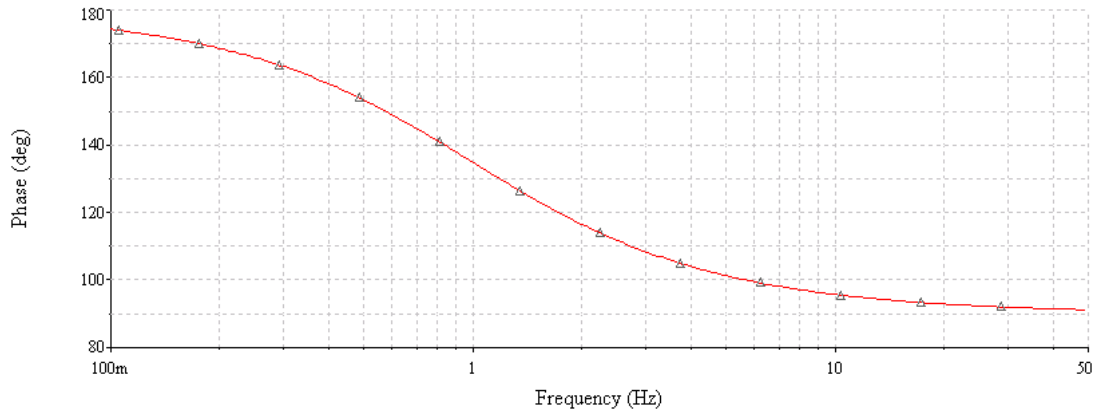


Figure 4.6: Phase Plot of the Frequency Response

A function generator was used to supply the integrator to show its performance at different frequencies. The integrator was supplied with square wave signals at different frequencies to represent the output signal of the accelerometer. The input voltage had an offset of 2.5V to represent the virtual ground of the accelerometer output signal. Figure 4.7 shows the input and output of the integrator operating at 10 Hz frequency.

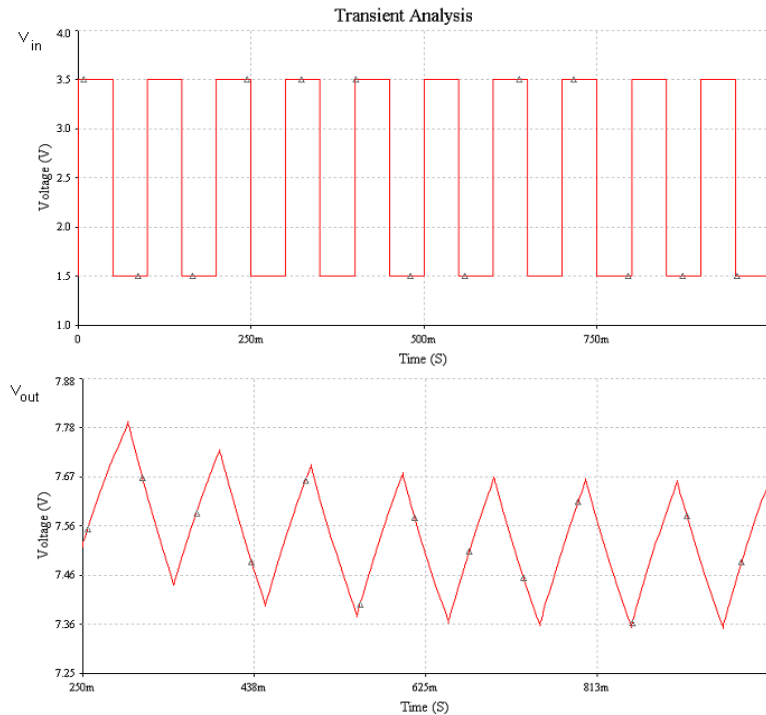


Figure 4.7: Input and Output Signals of the Integrator at 10Hz Frequency

As shown the integrator is able to produce a perfect triangular wave but the magnitude of the output waveform is greatly diminished. Figure 4.8 shows the output of the integrator when the input signal is a square wave at 0.8Hz.

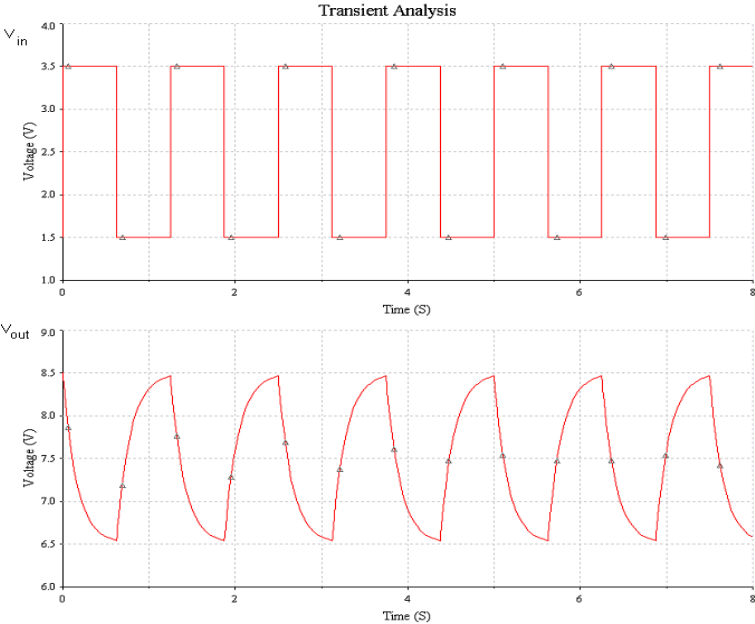


Figure 4.8: Input and Output Signal of Integrator at 0.8Hz Frequency

The quality of the output signal at 0.8 Hz is not as good as that at 10Hz because the capacitor is charging and discharging faster than the square wave is running. But increasing the value of the capacitor greatly reduces the magnitude of the output wave at 10Hz so we decided to keep the capacitor value at 200uF. Figure 4.9 shows the output of the integrator at a frequency halfway between the operating range 5Hz.

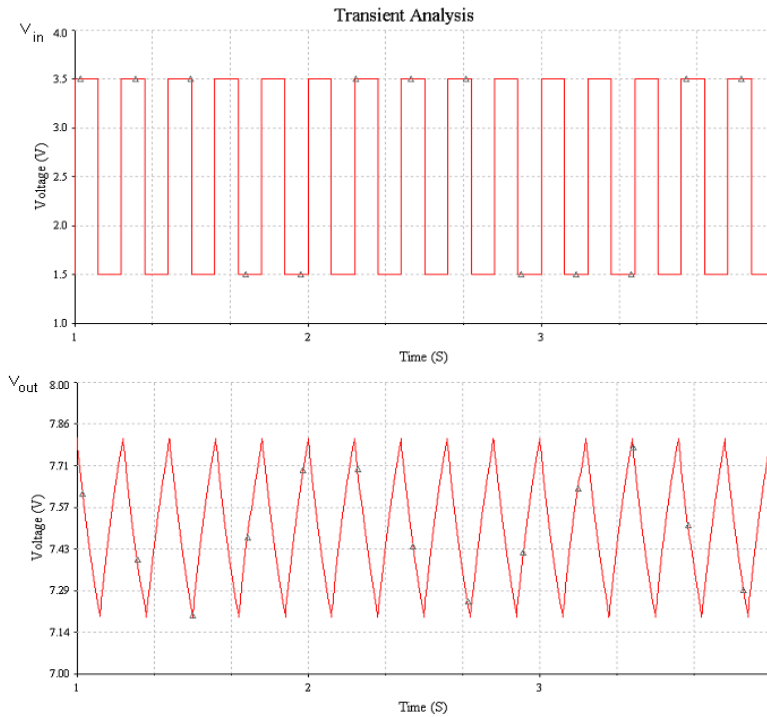


Figure 4.9: Input and Output Signal of Integrator at 5Hz Frequency

The integrator circuit was constructed and analyzed using the simulation program MULTISIM. Unfortunately; the actual construction of the circuit was unsuccessful. The signal from the accelerometer had much distortion and ranged in very low frequency which made the performance of the integrator inefficient. Therefore due to time consumption and after many tries the construction of the integrator was not concluded. The simulations performed in this part were valid and were used in the subsequent parts of this report.

5. Controller

The goal of the controller was to produce the desired action to completely eliminate the movement in the vehicle's body. In section 1 of this paper the suspension system was represented through two differential equations (1) and (2) and the electrical circuit shown in Figure 1.5. The damping coefficients, spring constants and the masses of the suspension system and vehicle's body were represented by resistors, capacitors and inductors respectively. The forced produced by the road condition $F(t)$, was the supply voltage of this circuit while the currents \dot{X} and \dot{Y} represented the vertical velocities the system moved. The circuit was simulated and the results in Figure 1.6 showed that the vehicle's body M_b will oscillate with a vertical velocity \dot{Y} for different road conditions and it took approximately 4 seconds for this velocity to go to zero which is a long time. These results confirmed that there is a need for a control signal that eliminates the movements of the vehicle's body and therefore keep the \dot{Y} as close to zero as possible. Figure 5.1 shows the circuit with the control source connected.

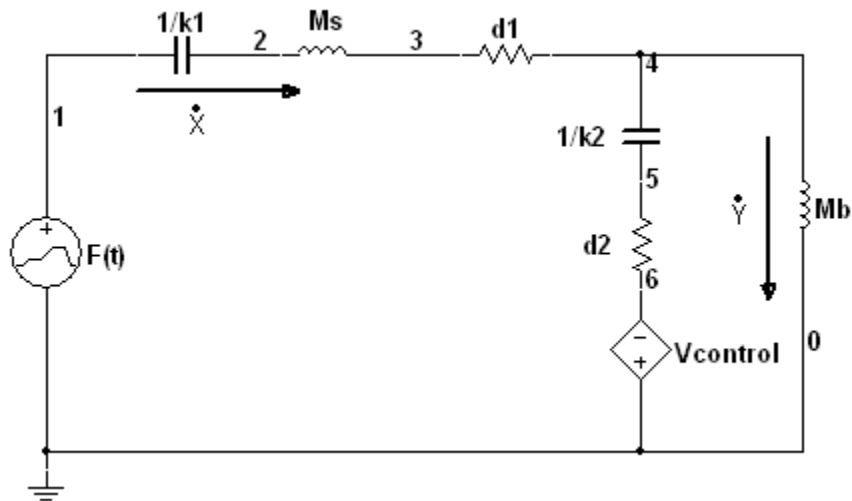


Figure 5.1 Electrical Representation of Suspension System

For the current in the inductor M_b to come to zero, the control voltage has to bring the voltage across it also to zero. In other words the $V_{control}$ source must supply a large enough voltage to create a short circuit in node 4 therefore making \dot{Y} go to zero. The

control voltage source will be dependent on the current \dot{Y} since it changes due to different road conditions $(F(t))$. Through different analysis of the circuit in Figure 5.1 it was concluded that the proportional controller circuit shown in Figure 5.2 will achieve the desired voltage.

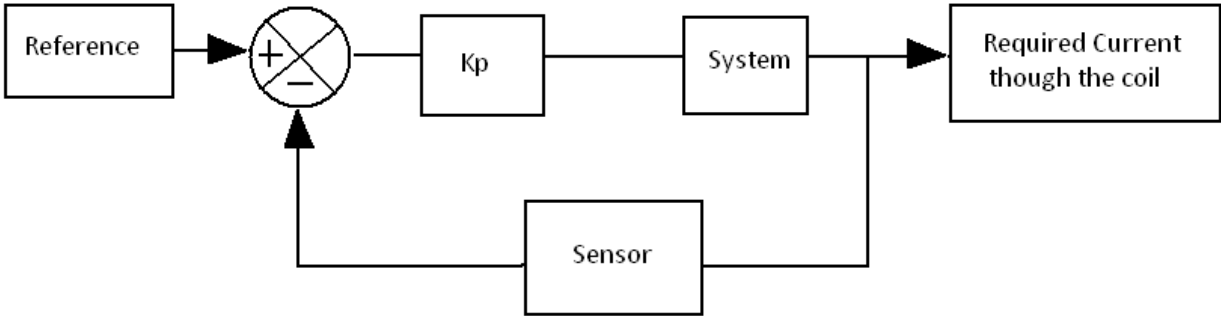


Figure 5.2: Controller

A proportional controller is a control loop feedback mechanism that attempts to correct the error between a measured variable and a desired set point. The controller will calculate and then output a corrective action that can keep the error recorded to a minimal. (9) The block diagram of the controller is shown in Figure 5.3.

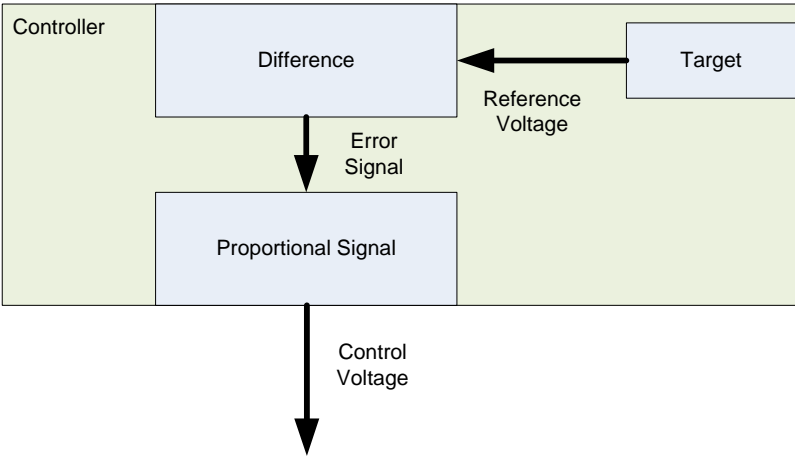


Figure 5.3: Block Diagram of Controller

The analysis and analog implementations of this type of controller are shown in the following sub-sections.

5.1. Difference Amplifier

As mentioned in the previous section the controller is used to correct the error between a measured variable and a desired set point. The desired set point for this suspension system is the zero movement of the vehicle's body. This means that the desired vertical velocity of Mb is zero. In Figure 5.3 this is represented as the target sub-module. The measured variable in this case is the actual vertical velocity the vehicle's body has due to different road conditions. The error signal is the difference between these two signals. Since the desired value of the velocity \dot{Y} is zero the error signal will than be the inverse of the recorded velocity \dot{Y} . This explain the reason of the Vcontrol source connection in Figure 5.1.

The error signal explained above will be applied only on the PSPICE simulations done to find Vcontrol. In reality the velocity calculated and produced by the signal conditioning module has a DC offset of 7.5V. The signal is also inverted by the integrator that obtained the velocity in this module. Therefore the signal produced by the signal conditioning module is the error signal used in this controller. The figure 1 circuit is simulated in PSPICE using Code 4.

Code 4:PSPICE Representation of Suspension System

```
Suspension System
Vroad 1 0 sin(0 1 3)
Ck1 1 2 0.000714285714
Lms 2 3 1.6
Rd1 3 4 10
Lmb 4 0 1.8
Ck2 4 5 0.000862068966
Rd2 5 0 15
Vcontrol 0 6 0

.PROBE
.TRAN 500ms 500ms 0 10m
.END
```

The Vcontrol source is connected in reverse due to its dependence on the inverse of current \dot{Y} . The Vroad source is the $F(t)$ of force produced to the suspension system by different road conditions. The circuit is supplied with a sinusoidal signal of amplitude 1V

and 3Hz frequency. The supply signal and the current through the suspension and body of the vehicles are shown in Figure 5.4.

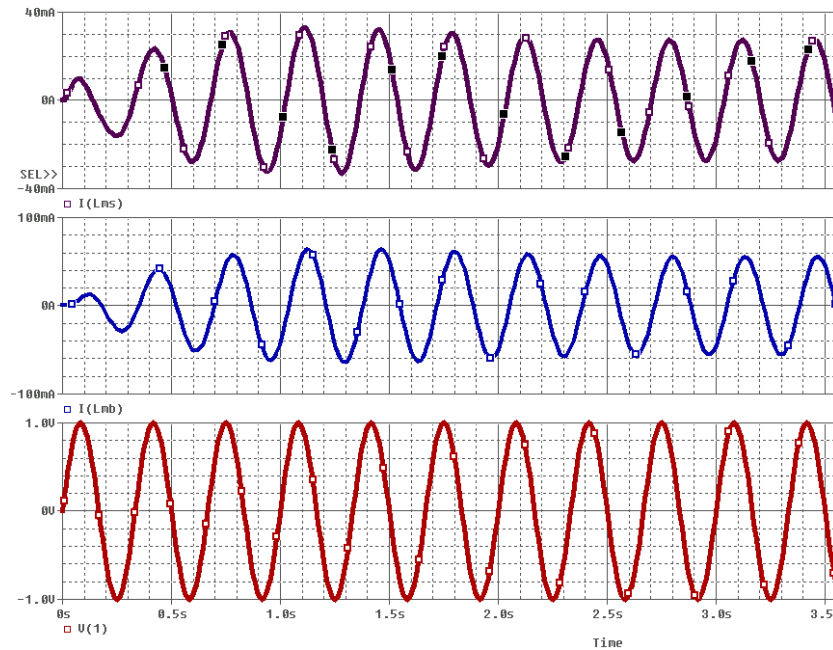


Figure 5.4: Velocities \dot{Y} I(Lmb) and \dot{X} I(Lms) due to Force $F(t)$ (V(1))

The simulation showed that when the system is supplied with a sinusoidal force of 1N peak with 3 Hz frequency the velocity of the oscillations in the vehicle’s body (Mb) will be up 0.063 m/s peak while the suspension system will have a velocity of 0.033m/s peak. The Vcontrol of Figure 5.1 was given the value of the error signal to see the change that it would have to the \dot{Y} velocity. The change in the PSPICE code is given in Code 5. The entire PSPICE code for this module is shown in appendix B.

Code 5: Control Source with Error Signal as Value

```
Econtrol 0 6 Value={I(Lmb)}
```

Since the Vcontrol is a dependent source the name in the PSPICE code had to change to Econtrol to eliminate errors in the program. The code shows that this source is given the value of the \dot{Y} current and connected in reverse to simulate the error signal. The results in the oscillation velocity of Mb were unnoticeable. This analysis concluded that the error signal obtained needs to be amplified to have any effect in the vertical velocity of the vehicle’s body.

5.2. Proportional Amplifier

The proportional amplifier sub-block will amplify the error signal to a certain value. The circuit used for this amplifier is shown in Figure 5.5.

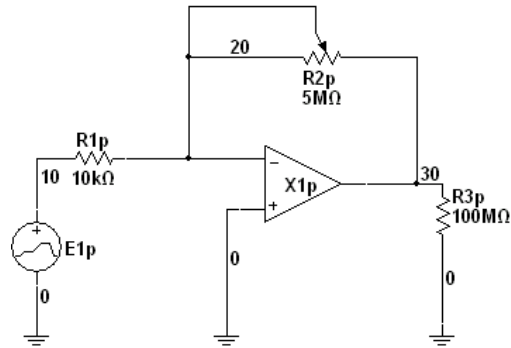


Figure 5.5: Proportional Amplifier Circuit

The circuit above is an inverting amplifier where E1p is the error signal and the resistors R1p and R2p are used to amplify the signal while R3p is used for reference. The output signal of this circuit is given from equation (8)

$$V(30) = K_p * V(10) \text{ where } K_p = -\frac{R_{2p}}{R_{1p}} \quad (8)$$

The PSPICE code of this circuit is given in Code 6.

Code 6: Proportional Amplifier

```
*Proportional Amplifier
E1p 10 0 value={I(Lmb)}
R1p 10 20 10k
R2p 20 30 RMOD 1
X1p 0 20 30 OPAMP
R3p 30 0 100MEG
*Determine the different constants
.MODEL RMOD RES(R=1)
.STEP RES RMOD(R) 10k, 5000k, 1000k
```

Code 6 is added to the PSPICE Code 4 to display the performance of the suspension system after the modifications to the error signal. The resistor R2p was changed as a potentiometer to determine the constant Kp that will reduce the \dot{Y} current the most. This resistor starts at 10kΩ and goes up to 5MΩ by a step of 1000. This will make the Kp constant start from 1 and go up to 400 with a step of 100. Due to the fact that the

proportional amplifier inverts the error signal while amplifying it the Vcontrol connections in Figure 5.1Error! Reference source not found. change directions. The output voltage signal obtained from the proportional amplifier is now used as the Vcontrol voltage. Also the input signal was change to a step input to better determine which Kp to use. This code changes are shown in Code 7.

Code 7: New connection and value of Vcontrol

```
Vroad 1 0 PULSE(0V 1V 1s 1us 1us 20s 40s)
Econtrol 6 0 Value={V(30)}
```

The simulation of the vertical velocity of the vehicle's body \dot{Y} for different values of Kp is shown in Figure 5.6.

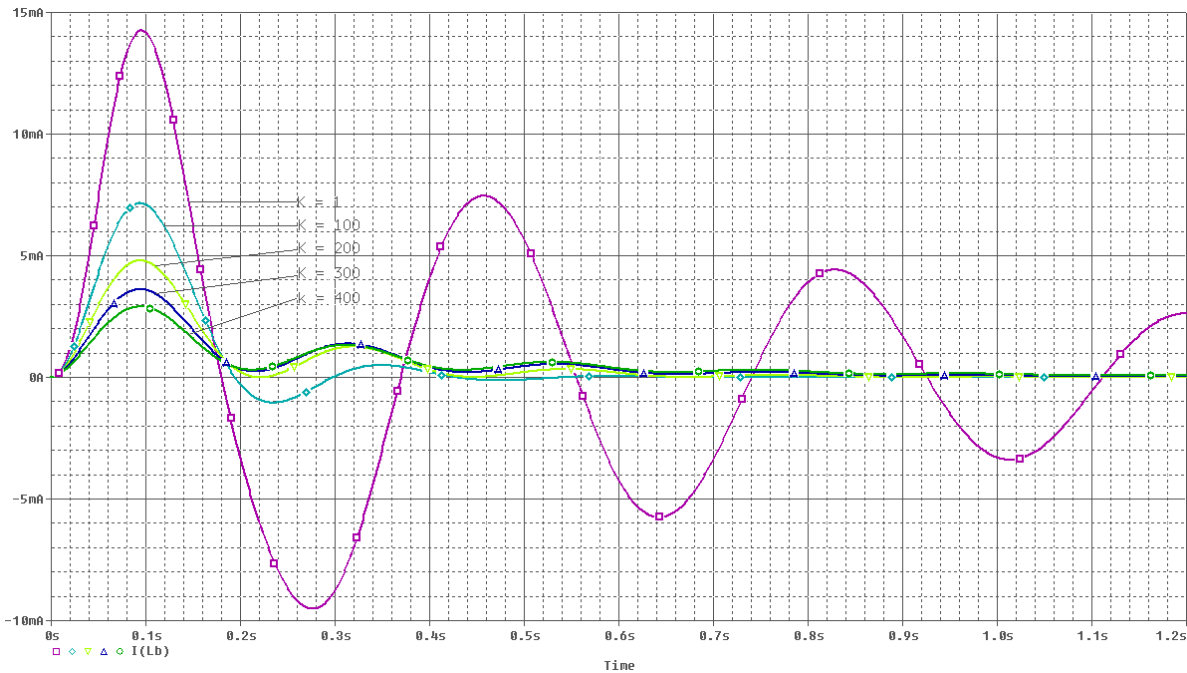


Figure 5.6: Vertical Velocity \dot{Y} of Vehicle's Body

The results show that the higher the Kp value the smaller the oscillations of the vehicle's body. The value of Kp was chosen to be 400. This means that the R2p resistor was chosen to be 4 MΩ. The vertical velocities of the suspension system and vehicle's body and the force F(t) supplied by the road condition are shown in Figure 5.7.

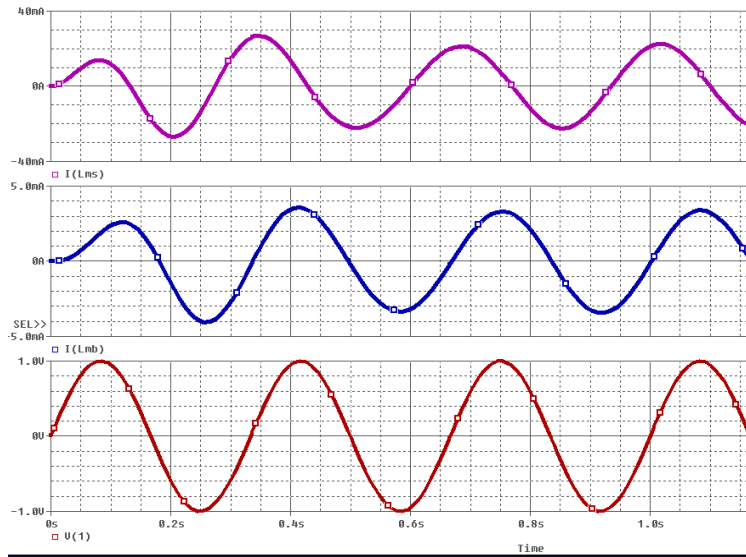


Figure 5.7: Input Voltage $V(1)$ ($F(t)$) and Currents through M_s $I(Lms)$ and M_b $I(Lmb)$

The vertical velocity \dot{Y} of the vehicle's body in **Error! Reference source not found.** after the proportional amplification was reduced to 0.003 m/s which is 21 times smaller than 0.063 m/s which is the velocity without the control action. To summarize the controller circuit the simulations of the input voltage, the control voltage and the current through the vehicle's suspension and body are shown in Figure 5.8, Figure 5.9 and Figure 5.10.

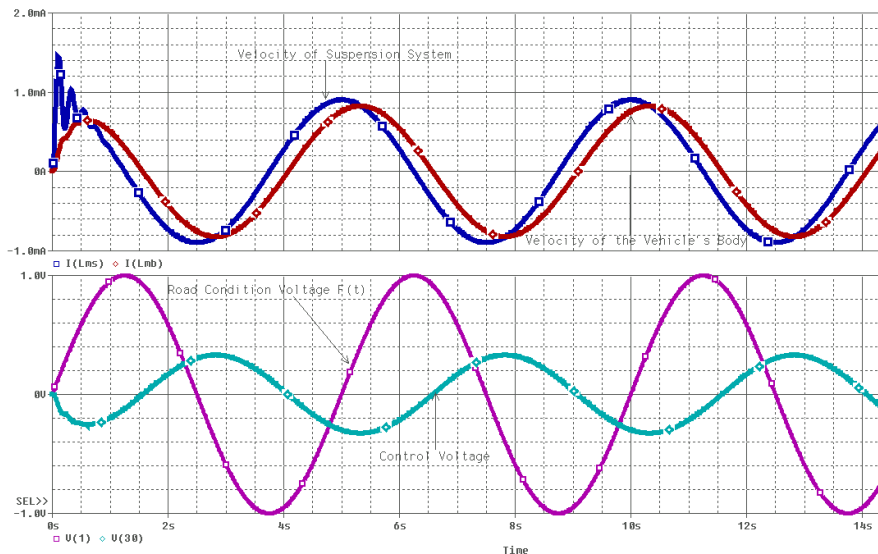


Figure 5.8: Suspension System Signals at 0.2Hz Frequency

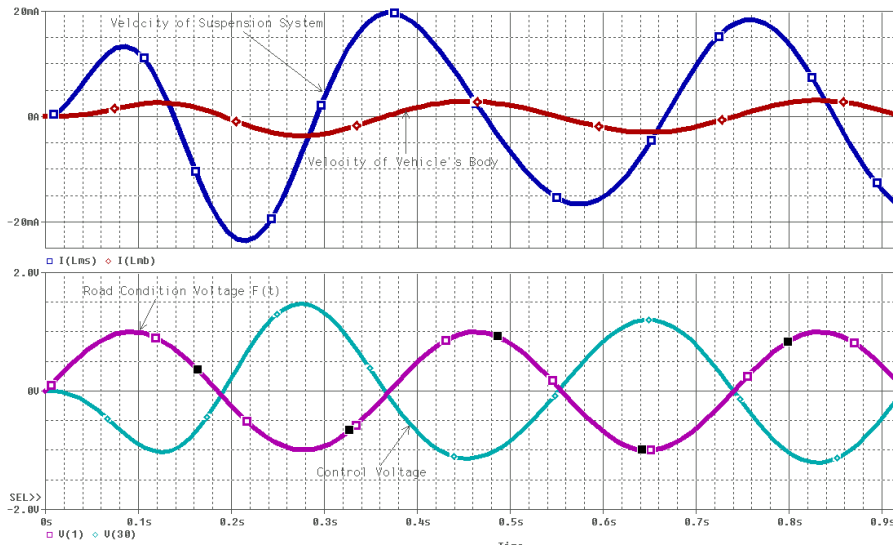


Figure 5.9: Suspension System Signals at 2.7 Hz Resonance Frequency

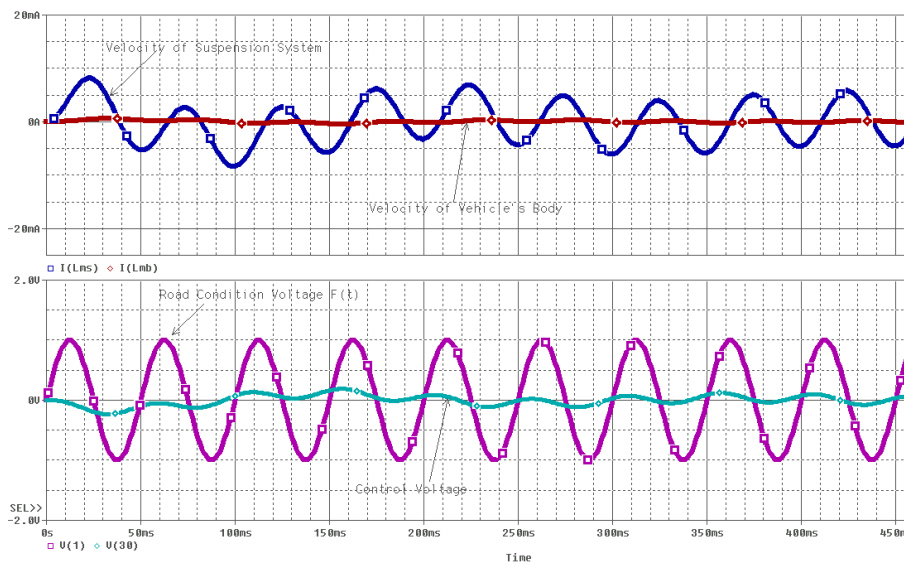


Figure 5.10: Suspension system at 20 Hz Frequency

The control signal $V_{control}$ produce by this module will have a maximum value of 1.5V when the input signal is 1V sinusoidal wave at resonance frequency of 2.7 Hz. The analog representation of the controller module is shown in Figure 5.11.

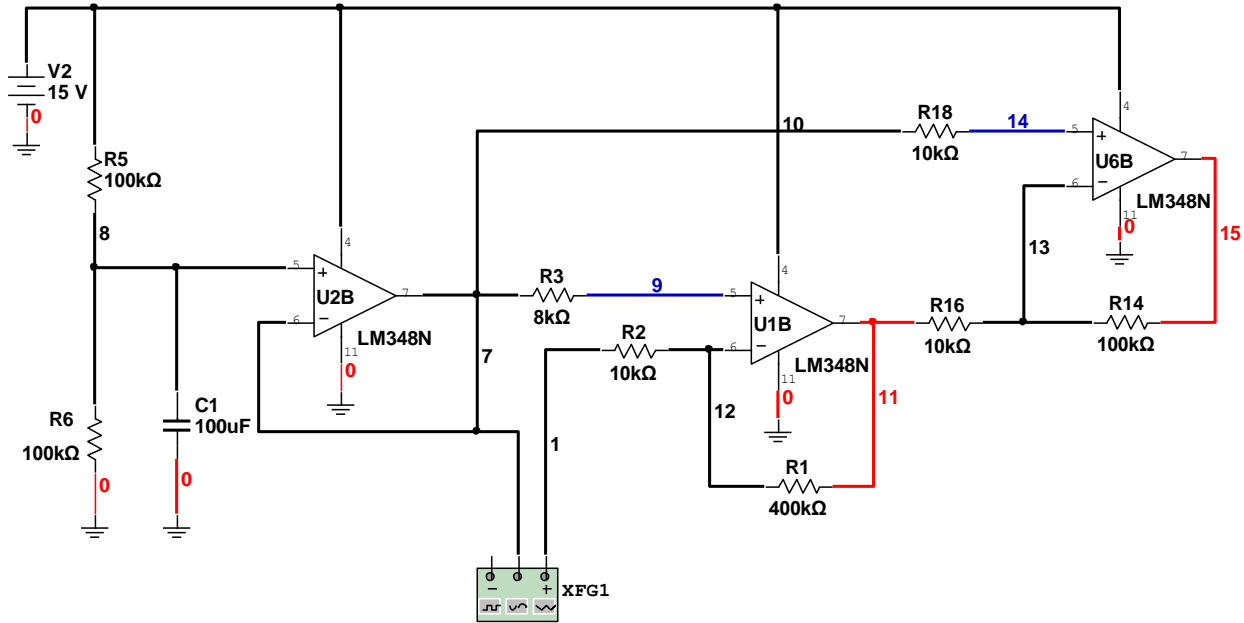


Figure 5.11: Analog Representation of Controller Module

The controller was built using LM348 Op-Amps as shown in Figure 5.11. To avoid using two independent supplies to power the controller, the circuit was designed so that it would run off 15V with a virtual ground set at 7.5V.

To obtain the virtual ground, a voltage divider was used. Large resistor values (100KΩ) were used in this case to reduce the amount of power dissipation. However, the large resistors produce a lot of high frequency noise. Therefore the 100nF capacitor was used to filter the noise created by these resistors. The op-amp U2B acts as a voltage follower.

A function generator was used to obtain the error signal since the circuit in Figure 5.11 does not include the feedback mechanism. The error signal was passed through two inverting amplifiers which amplified it by a magnitude of 400 which is the value of K_p obtained before. The purpose of cascading two amplifiers was to produce a non inverted error signal and also to limit the amount of amplification in a single stage. This will prevent the distortion of the signal by the amplifiers. The magnitude of the amplification by the controller can be obtained by equation (9).

$$K_p = \left(\frac{R_1}{R_2}\right) \times \left(\frac{R_{14}}{R_{16}}\right) = \frac{400K\Omega}{10K\Omega} \times \frac{100K\Omega}{10K\Omega} = 400 \quad (9)$$

6. Current Driver

The controller output signal is now used by the current driver module to supply the damper coil with the required current to keep the vehicles' body stable over time. The controller signal is fed to a pulse width modulator (PWM) where it is compared with a triangular wave signal produced by an oscillator. This oscillator is described in detail in the next section. The PWM will supply the H-Bridge with the appropriate pulse drive voltage to control the current supplied to the damper coil. Each of these sub-modules is also explained in detail in the subsequent sections. The circuitry that was used to achieve this goal is summarized in the block diagram shown in Figure 6.1.

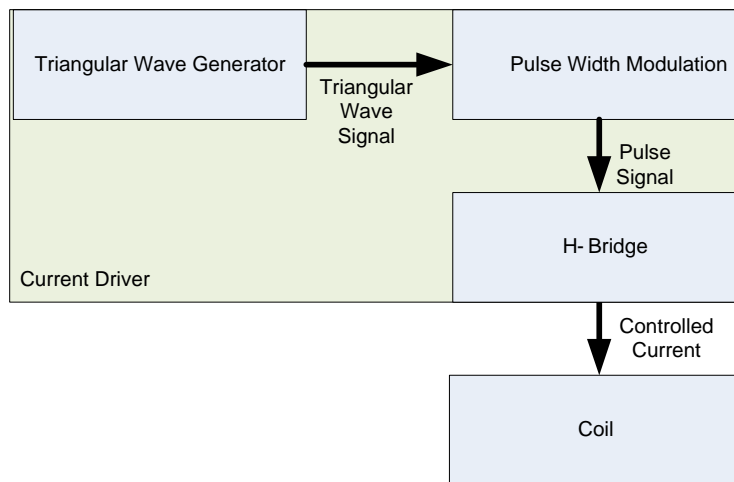


Figure 6.1: Current Driver Block Diagram

6.1. Triangular Wave Oscillator

To produce the necessary drive voltage the PWM needs to compare the control voltage from the controller to a triangular wave. To generate this triangular wave the circuit in Figure 6.2 was built. This triangular wave generator uses a 555-timer to produce a square wave which is then passed through an integrator circuit to obtain the necessary triangular wave.

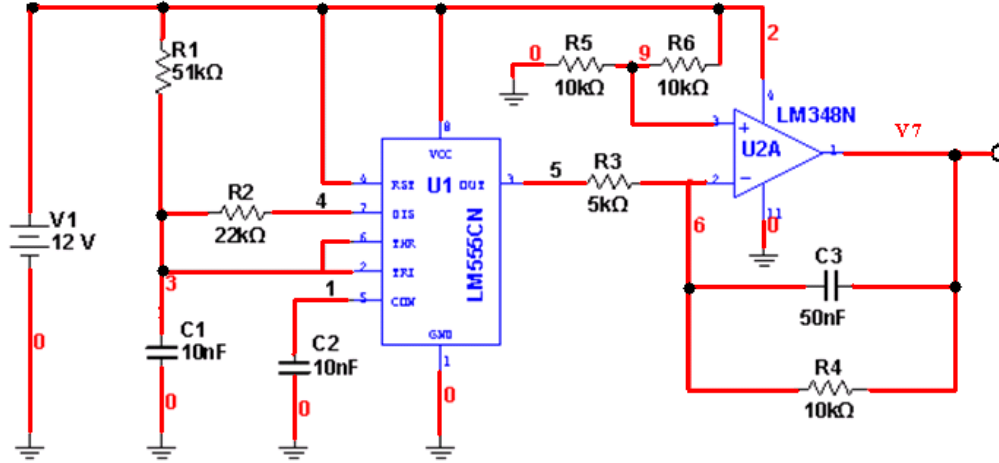


Figure 6.2: Triangular Wave Generator

The 555-timer is connected to generate a square wave of approximately 50% duty cycle. The duty cycle and frequency of the 555-timer is controlled by the R_1 and R_2 resistors and the capacitor C_1 . The output signal has to have a high frequency for accurate simulations of PWM module. The output can be controlled by the expressions defined in equation (10), (11) and (12). Equation (10) defines the time for highest voltage point for the rectangular wave. Equation (11) defines the period for the lowest voltage point for the rectangular wave. Equation (12) expresses the frequency of the rectangular wave. (8)

$$t_1 = 0.693 * R_1 * C \quad (10)$$

$$t_2 = \left[\frac{R_1 * R_2}{R_1 + R_2} \right] * C * \ln \left[\frac{R_2 - 2R_1}{2R_2 - R_1} \right] \quad (11)$$

$$f = \frac{1}{t_1 + t_2} \quad (12)$$

The components values used produced an output rectangular wave with $t_1 = 0.3534\text{ms}$, $t_2 = 0.3744\text{ms}$ and $f = 1.37\text{kHz}$. Equation (13) is used to calculate the duty cycle of this circuit.

$$D = \frac{t_1}{t_1 + t_2} \quad (13)$$

Therefore, the duty cycle of the output signal of the 555 timer is $D = 0.4856 \approx 49\%$ which is extremely close to the desired 50% duty cycle. The output generated by the 555-

timer is shown in Figure 6.3. The amplitude of the output signal is 12V which is the same voltage V_{cc} required to power up the 555-timer. The figure also shows that the output signals high and low periods are identical. This rectangular wave is then fed into an integrator circuit which converts this signal to obtain the desired triangular wave.

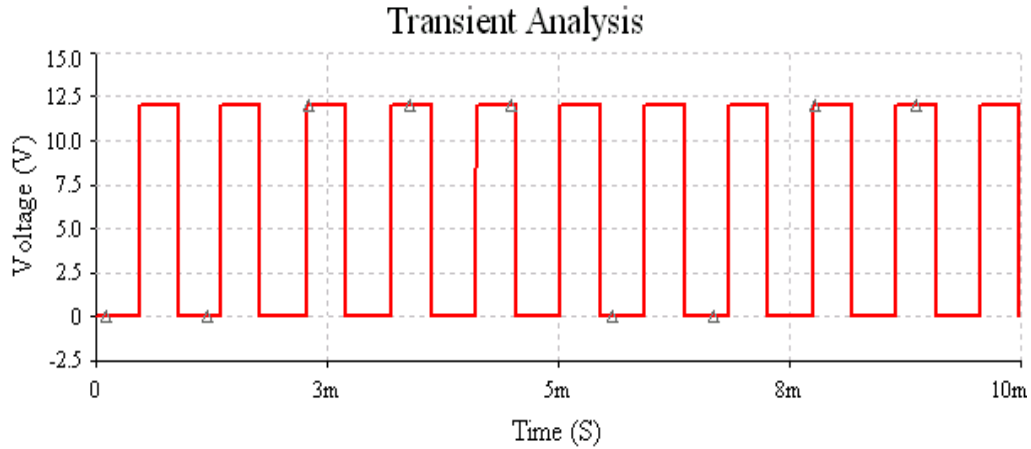


Figure 6.3: 555-Timer Output

The LM348N op-amp is used for the integrator circuit to obtain the desired output signal. The positive input of the op-amp is connected to a reference voltage of 6V produced by the voltage divider network R_5 and R_6 . This reference voltage was chosen so that the output triangular wave has the same DC offset as the control signal from the controller. This way the PWM will produce an accurate output to drive the H-Bridge. The capacitor value for C_2 was chosen to be 50nF due to the high frequency of the 555-timer output. The resistor R_4 controls the DC gain of the output. Figure 6.4 shows the output signal of the final triangular wave oscillator sub-module.

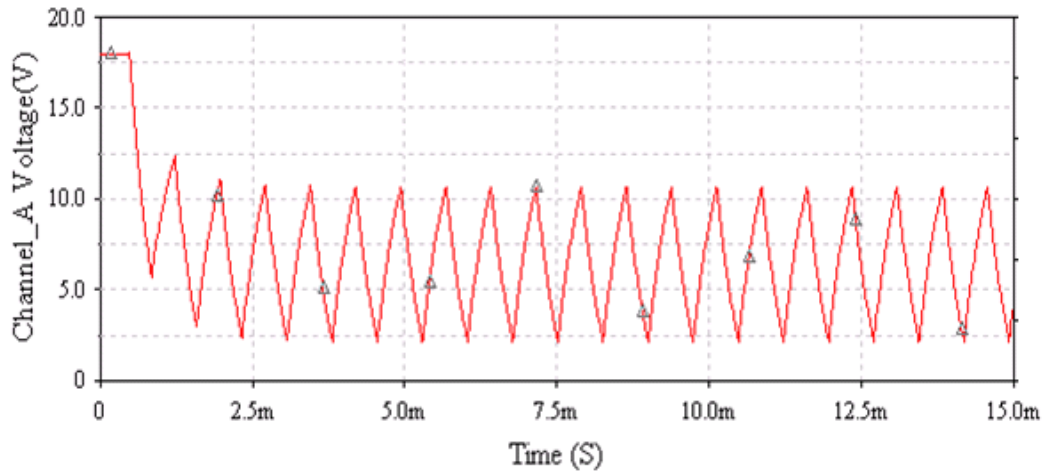


Figure 6.4: Output of Triangular Wave Oscillator

6.2. Pulse Width Modulation

The pulse width modulation sub-module compares the control signal of the controller with the triangular wave produced by the oscillator. The output signal will control the H-Bridge current flow for the damper coil. Figure 6.5 shows the schematic of this sub-module.

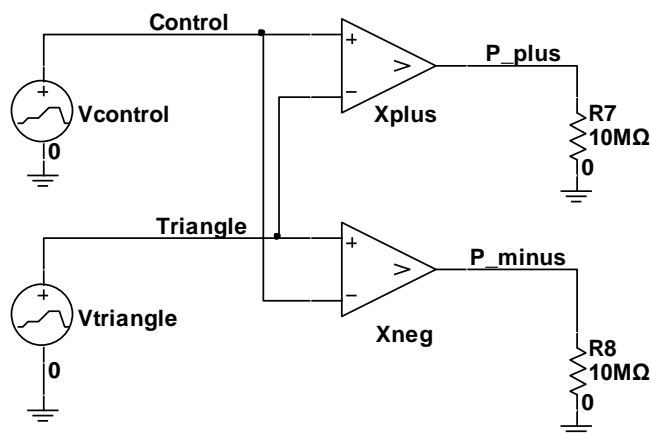


Figure 6.5: Schematic of PWM Module

The output of comparator Xplus goes high every time the triangular signal is greater than the control signal, otherwise it's low. For the complete operation description of the comparator, please refer to Section 3.1.1. The output of comparator Xneg is opposite to the

output of comparator Xplus. The circuit was simulated using the PSPICE program. The generated code presented in Code 8 shows the representation of this circuit in PSPICE.

Code 8: PWM

```
*****
* OPAMP MACRO MODEL, SINGLE-POLE *
* connections: non-inverting input *
* | inverting input *
* | | output *
* | | | *
.SUBCKT OPAMP P N T1 ;*
Rin P N 100MEG ;*
Ea A 0 TABLE {V(P,N)} = 0,0 1u 10 1000,10 ;*
; *
Rc A T1 100 ;*
Co T1 0 1000p ;*
ROUT T1 0 10MEG ;*
; *
.ENDS ;*
*****

*THIS SECTION WILL GENERATE PULSES FOR H BRIDGE

Vtriangle Triangle 0 PULSE(2.5V 10V 0s 0.365ms 0.365ms .001ps 0.73ms)
Voffset Offset 0 6.75V ;DC offset
Vcontrol Control Offset SIN(0V 3V 100Hz)
Xplus Control Triangle P_Plus OPAMP
Xneg Triangle Control P_minus OPAMP
Rplus P_plus 0 10MEG ;positive pulse output
Rneg P_minus 0 10MEG ;negative pulse output

.PROBE
.TRAN 10m 10m 0 1m
.END
```

The code labeled macro model represents the comparators used Figure 6.5. The triangular signal (Vtriangle) is simulated identical to the one obtained from the triangular wave generator. The controller signal (Vcontrol) is simulated as a sinusoidal wave with a magnitude of 3V at a frequency of 100Hz and a DC offset (Voffset) of 6.75V. The frequency of Vcontrol is set to 100Hz for simulation purposes. Due to the high frequency of the triangular wave the simulation is processed for 10mS. Figure 6.6 shows the input and outputs signals of the PWM sub-module. The P_plus signal is the output of comparator Xplus while P_minus is the output of comparator Xneg. The simulations proved that the PWM module works as desired. These output signals are then used to control the current flow of the H-bridge.

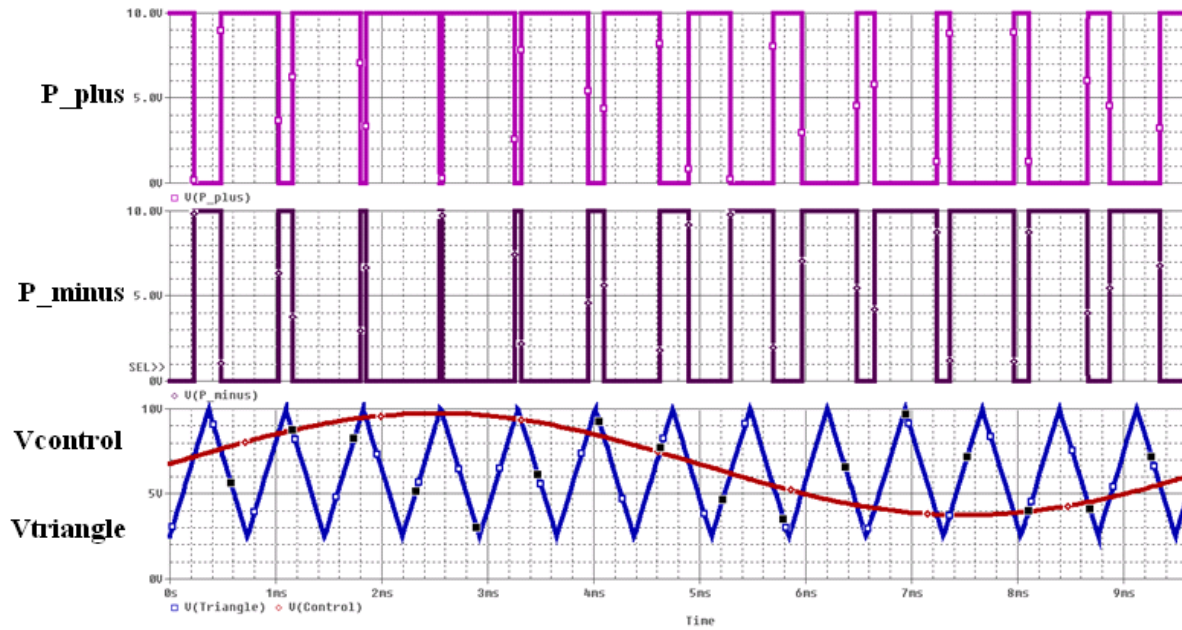


Figure 6.6: Output and Input Signal of the PWM

6.3. H-Bridge

The pulse signals P_plus and P_minus are used to control the current flow through the H-Bridge. The H-Bridge circuit allows to acquire a bipolar current flow through the damper coil when the pulse signals are applied to it as it is shown in Figure 6.7 schematic.

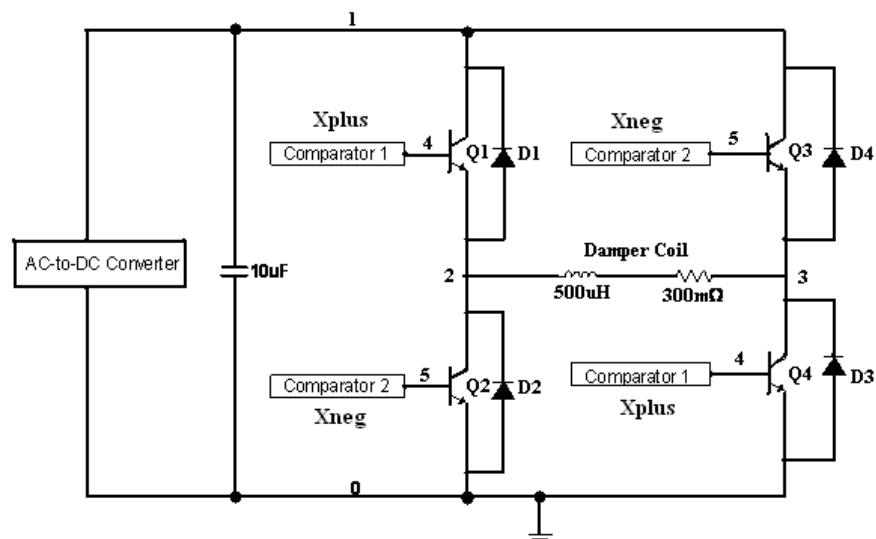


Figure 6.7: H-Bridge Circuit

The circuit was built using power transistors capable of withstanding currents greater than 15A. Transistors Q₁ and Q₄ are driven by the signal from the comparator Xplus while transistors Q₂ and Q₃ are driven by the signal from comparator Xneg. Q₁ and Q₄ are turned on when the pulse signal P_plus is applied to both while Q₂ and Q₃ are turned off. This forces the current through the coil to flow in a clockwise direction. On the other hand, Q₂ and Q₃ are turned on when the pulse signal P_minus is applied to both while Q₁ and Q₄ are turned off. This forces the current through the damper coil to flow in an anticlockwise direction. However; the current that flows through the coil does not follow the same curve as the control voltage due to the internal resistance and the inductance of the damper coil. These values were obtained in Section 1 and in Section 3.2.2. They generate a small time delay t_{delay} between the voltage and the current curves in the H-Bridge. The time delay is defined as the ratio of the damper coil inductance and its internal resistance as it shown in Equation (14).

$$t_{delay} = \frac{L}{R} = \frac{500\mu H}{300m\Omega} = 1.667mSeconds \quad (14)$$

Diodes are connected across the transistors to allow a flow of any residual current during switching performance of the H-Bridge. The transistors used to build this circuit are the same Darlington BJTs as the one used in the excitation coil of the road condition module. Figure 6.8 shows the connections of these transistors to form the H-Bridge circuit.

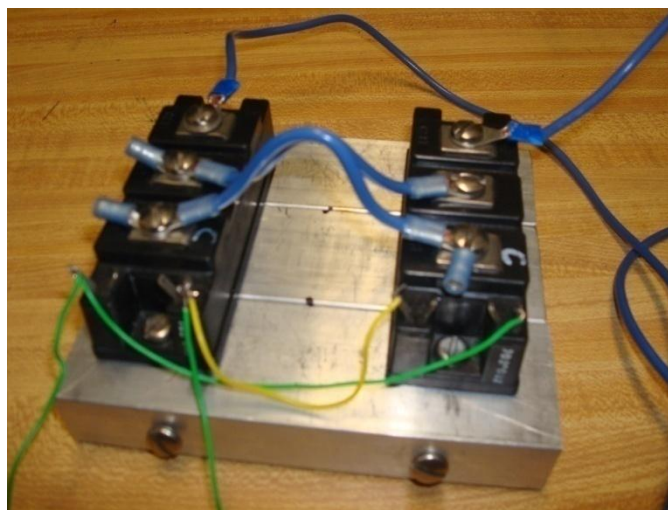


Figure 6.8: H-Bridge Connections using the Darlington BJTs

The PSPICE program was used once again to simulate the behavior of the H-Bridge circuit. The generated code is labeled Code 9 as it is subsequently shown.

Code 9: H-Bridge Representation in PSPICE

```
*****
* H-BRIDGE WITH DIODES CONNECTED ;*
; *
* CONNECTIONS: POSITIVE TURMINAL ;*
* | NEGATIVE TURMINAL ;*
* | | TRANSISTER 1 ;*
* | | | TRANSISTER 2 ;*
* | | | | TRANSISTER 3 ;*
* | | | | | TRANSITER 4 ;*
* | | | | | | ;*
* | | | | | | | ;*
.SUBCKT H_BRIDGE M1 M2 Y1 Y2 Y3 Y4 ;*
; *
S1 10 M1 Y1 0 PTRA ;*
S2 M1 0 Y2 0 PTRA ;*
S3 10 M2 Y3 0 PTRA ;*
S4 M2 0 Y4 0 PTRA ;*
.MODEL PTRA VSWITCH (RON=1U ROFF=10MEG VON=.1) ;*
; *
** DIODE CONNECTIONS ;*
; *
DQA 0 M1 DIODE ;*
DQB M1 10 DIODE ;*
DQC 0 M2 DIODE ;*
DQD M2 10 DIODE ;*
.MODEL DIODE D(N=.0001 RS=2U BV=120000) ;*
; *
*DC VOLTAGE CONNECTED TO THE H-BRIGE ;*
CFILTER 10 0 10u ;*
VBIAS 10 0 6V ;*
.ENDS ;*
```

The transistors of the H-Bridge are represented as switches in the PSPICE code. The DC voltage that supplies the transistors is chosen to be 6V since the desired current needed in the dumber coil is ±20A. The 6V voltage is supplied to the H-Bridge by an AC-to-DC converter which is described in the next section. The code generated to simulate the connections between the PWM output signals and the H-Bridge is expressed in Code 10.

Code 10: PWM and H-Bridge Connections

```
*THIS SECTION CONNECTS THE H-BRIDGE
*-----
Xbridge M1 M2 P_Plus P_minus P_minus P_Plus H_BRIDGE
Lcoil M1 B1 0.5m
Rcoil B1 M2 0.3
```

To obtain more realistic results from the simulation, the control signal frequency was changed from 100Hz to 10 Hz. The simulation was performed for about 500ms and the results are shown in Figure 6.9. The simulations showed that the H-Bridge circuit worked as desired. However; there is a small ripple in the current signal but its frequency is much higher than the control signal frequency therefore it has a negligible effect in the performance of the system. This proves that the control signal provided by the controller is successfully transformed into the required current needed by the damper coil to keep the vehicle's body in a constant state regardless of the road conditions. The complete PSPICE code of the PWM and H-Bridge connections is shown in appendix B.

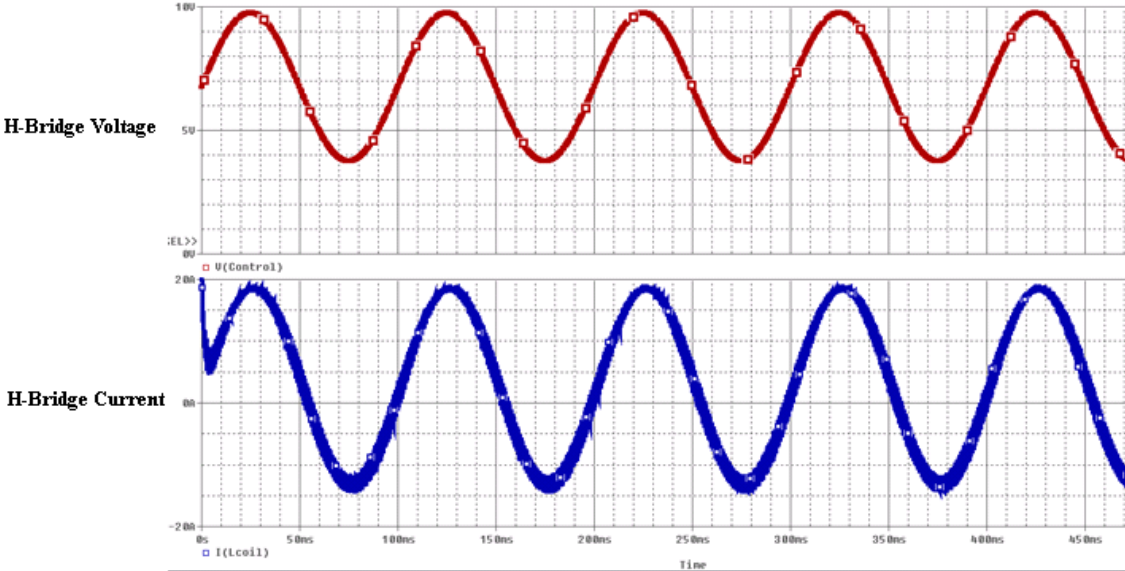


Figure 6.9: Control Signal V(control) and Control Current of damper coil

7. AC to DC Converter

Through the construction of the road condition module it was discovered that the coils need about 20A to interact with the magnets of our model. At first a power supply capable of supplying this current was used to drive both coils. This produced problems because when it was used to power the excitation coil used in the road condition module, the supply voltage was dropping down from 15V to about 5V every time the Darlington BJT allowed current through the coil. Therefore the same power supply could not be used for the H-Bridge which produces the counter force to keep the vehicle's body from moving. To solve this problem an AC to DC converter was build that generates the power supply needed using the wall outlet. The block diagram of this circuit is shown in Figure 7.1.

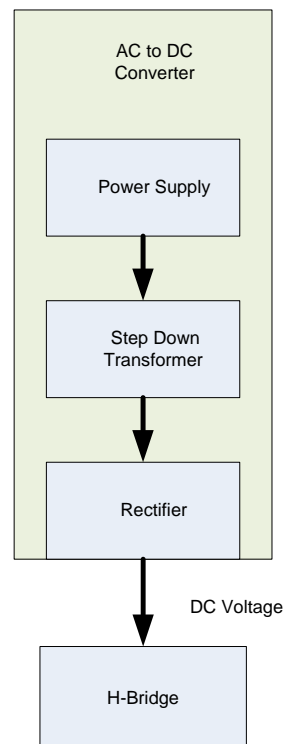


Figure 7.1: AC-to-DC converter Block Diagram

The block diagram shows that the signal coming from the wall outlet is then supplied to a step down transformer which reduces the voltage and amplifies the current to the desired values. This signal is then supplied to a rectifier circuit to transform it to a DC signal. The DC voltage signal supplies the H-Bridge with the appropriate amount to drive

the damper coil. The step down transformer and the rectifier circuit are explained in the following subsection.

7.1. Transformer and Rectifier

The transformer used in this module is a POWERSTAT Variable Transformer. These transformers take in utility lines voltage and produce controllable output voltages. *“They provide excellent power regulation with negligible variation in output voltage from no-load to full-load current.”* (9) The POWERSTAT used in this application is the 136B series shown in Figure 7.2.



Figure 7.2: POWERSTAT Transformer

This transformer takes in the 120V and produces a desired output voltage. The rating chart for this type of transformer is shown in Figure 7.3.

RATINGS CHART

120 VOLT, SINGLE PHASE																						
"LINE" CONNECTION						"BOOST" CONNECTION						"STEP-UP" CONNECTION										
Input Voltage:		120				120						N/A										
Output Voltage:		0-120				0-140																
Constant Current Load		Constant Impedance Load		Terminals & Rotation		Constant Current Load		Terminals & Rotation		Constant Current Load		Terminals & Rotation		Model Numbers								
Freq. (Hz)	Max. Amps	Max. KVA	Max. Amps	Max. KVA	Input CW CCW	Output CW CCW	Jumper CW CCW	Freq. (Hz)	Max. Amps	Max. KVA	Input CW CCW	Output CW CCW	Jumper CW CCW	Freq. (Hz)	Max. Amps	Max. KVA	Input CW CCW	Output CW CCW	Jumper CW CCW	Manually Operated	Motor Driven	Conn. Diag.
50/60	20	1.8			1-4 1-4	1-3 3-4		50/60	20	1.8	1-2 4-5	1-3 3-4										7
50/60	22	2.6	28	34	1-4 1-4	1-3 3-4		50/60	22	3.1	1-2 4-5	1-3 3-4										1
50/60	44	5.3	5.6	6.7	1-4 1-4	1-H2 4-H2	1-1, 4-4 1-1, 4-4	50/60	44	6.2	1-2 4-5	1-H2 4-H2	1-1, 2-2 4-4, 5-5									9
50/60	66	7.9	84	10.1	1-4 1-4	1-H2 4-H2	1-1, 4-4 1-1, 4-4	50/60	66	9.2	1-2 4-5	1-H2 4-H2	1-1, 2-2 4-4, 5-5									11

Figure 7.3: Rating Chart of POWERSTAT (9)

The simulations of this transformer were not possible to perform since there is no representation for it in the MULTISIM program. The simulations shown in this part take into consideration that the transformer produced the desired output.

To get the desired DC voltage the AC voltage obtained from the transformer is passed through a rectifier circuit. The rectifier circuit consists of four diodes connected in a bridge configuration with their correspondent heat sinks. This combination gives a full-wave rectifier which will produce a better DC signal. The diodes used in this circuit are the 1N3766 diodes which datasheet is shown in the appendix C. The rectifier circuit that was built to achieve the desired DC voltage is shown in Figure 7.4.



Figure 7.4: Rectifier Circuit

The circuitry of the transformer and rectifier has to meet certain specifications to produce the desired output. Some of these specifications are shown below.

Specification:

- Safety. Built in mechanism to prevent current surges.
- Able to provide a current of about 20A
- Output voltage ripple kept below 30% of the DC voltage

Calculations were made based on these specifications to derive the necessary components.

A capacitor is connected in parallel with the damper coil to keep the ripple of the output voltage below 30%. The resistance of the coil was measured to be about 0.3Ω. Since the current going through the coil needs to be around 20A the DC voltage required would be about 6V as Equation (15) shows.

$$R * A = 0.3\Omega \times 20A = 6V \quad (15)$$

Therefore the peak DC voltage required is obtained from Equation (16). In this case the $V_{dc} = 6V$ which will make $V_{peak} = 9.424V$

$$V_{dc} = \frac{2V_{peak}}{\pi} \quad (16)$$

Since the capacitor is connected in parallel with the coil it will have the same voltage. If the ripple voltage is assumed to be a saw tooth wave the value of the capacitor is estimated using Equation (17). The $V_{r_{RMS}}$ is the rms value of the ripple voltage. The wall outlet will provide a signal with a frequency of 60Hz. In this case R_L is the coil resistance which is 0.3 Ω. Solving Equation (17) for C, the value of the capacitor needed to achieve this ripple is $C \approx 27mF$. (11)

$$\frac{V_{r_{rms}}}{V_{dc}} = \frac{1}{4\sqrt{3}R_L f C} = 30\% \quad (17)$$

For safety reasons a fuse is connected in the primary coil of the transformer to limit the current surges. To select the fuse for this application it is necessary to know the current that flows through the primary coil of the transformer. For this calculation an ideal

transformer was assumed. Equation (18) is used in this case to calculate the current I_p in the primary coil.

$$\frac{N_p}{N_s} = \frac{I_s}{I_p} = \frac{V_p}{V_s} = \frac{120}{9.42} = 12.7 \quad (18)$$

The primary voltage supplied by the wall outlet is 120V peak. Since $I_s = 20A$ DC, its peak value is calculated using Equation (16) except replacing the voltage values by current values.

$$I_{sPeak} = 20A \times \frac{\pi}{2} = 31.4A$$

Now using Equation (18) the primary peak current will be about 2.47A as it is shown in the calculations performed.

$$I_{pPeak} = \frac{I_s}{12.7} = \frac{31.4}{12.7} = 2.47 A$$

Therefore the I_{RMS} current that will be flowing through the primary is about 1.75A. From these calculations a 2A fuse was chosen to limit the current surge in the primary coil of the transformer.

$$I_{RMS} = \frac{I_p}{\sqrt{2}} = 1.75A$$

The complete circuit schematic of the transformer and rectifier connected with the calculated component values are shown in Figure 7.5. In the figure the internal resistance of the damper coil is represented by the R1 value while C_1 is the capacitor calculated previously.

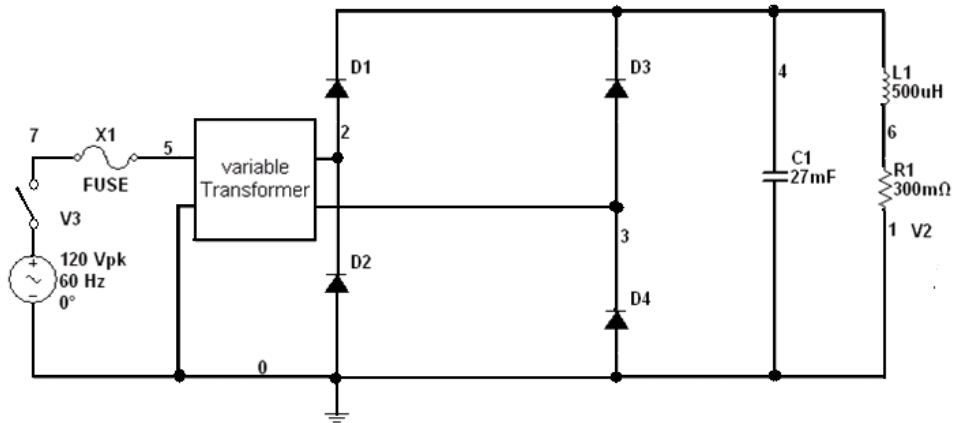


Figure 7.5: AC-to-DC Converter

The transient analysis of the output voltage and the output current of this circuit are shown in Figure 7.6 and Figure 7.7. The simulations performed showed that the desired voltage and current was obtained from the circuit. The ripple maintained was kept at a 30% value by the capacitor used. These signals will supply the H-Bridge circuit of the current driver which will control the current that flows through coil-2 of the model.

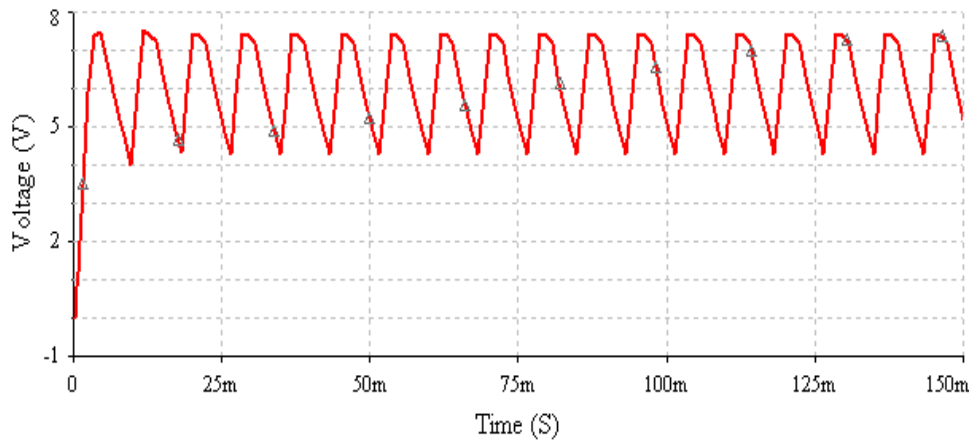


Figure 7.6: Output Voltage of the AC-to-DC Converter

Transient Analysis

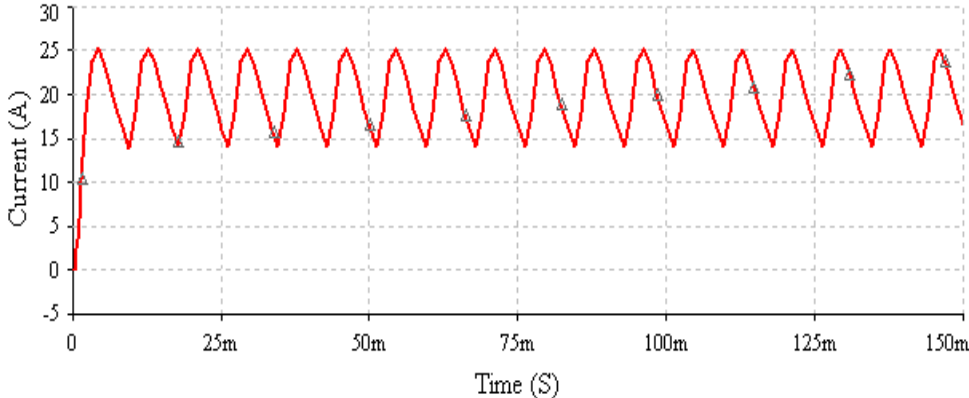


Figure 7.7: Output Current of the AC-to-DC Converter

8. Conclusion

Due to the inefficiency of the current suspension systems, the main goal of this project was to design a more efficient suspension system. After a careful evaluation it was found that a dynamic electromagnetic suspension system performs the tasks established to accomplish this goal.

Once the mechanical system was designed and built, the equivalent electrical circuitry was derived to analyze and implement the design. This helped to attain a block diagram to further simplify the necessary steps to achieve the main goal. The block diagram helped establish the specific modules needed to achieve the desired behavior of the system. The main modules of the block diagram were identified as the Road Condition, Signal Conditioning, Controller, Current Driver and the AC-to-DC Converter.

The road condition module was able to generate a triangular wave at different frequencies and amplitudes. The frequency and the amplitude were manually adjusted by the operator to manipulate the current flow through the coil connected in series with the BJT transistor. The result of this module showed similar effects to that of uneven road conditions.

The signal conditioning module easily measured the model's acceleration with the use of a highly sensitive accelerometer. An optimal velocity signal was obtained by feeding this signal to an integrator circuit. The overall result was an accurate and useable velocity signal as it was shown in the corresponding section.

The controller module manipulated this velocity signal to obtain the necessary signal to achieve the main goal. The signal was inverted, amplified and integrated to reach the appropriate conditions. The controller simulation output behaved as expected since all of the sub-modules circuitry were simple to design and implement.

The current driver module was able to supply the appropriate current to the coil to keep the vehicles body stable. The signal was modified to drive a H-Bridge in the correct way through the use of a pulse width modulator to achieve the needed current. The H-Bridge circuit showed excellent results.

The AC to DC converter circuit transformed the wall outlet voltage to the necessary values used by damper coil of the mechanical system. The 120 V signal was converted to the desired value used to supply our circuit through the use of a step-down transform and a rectifier.

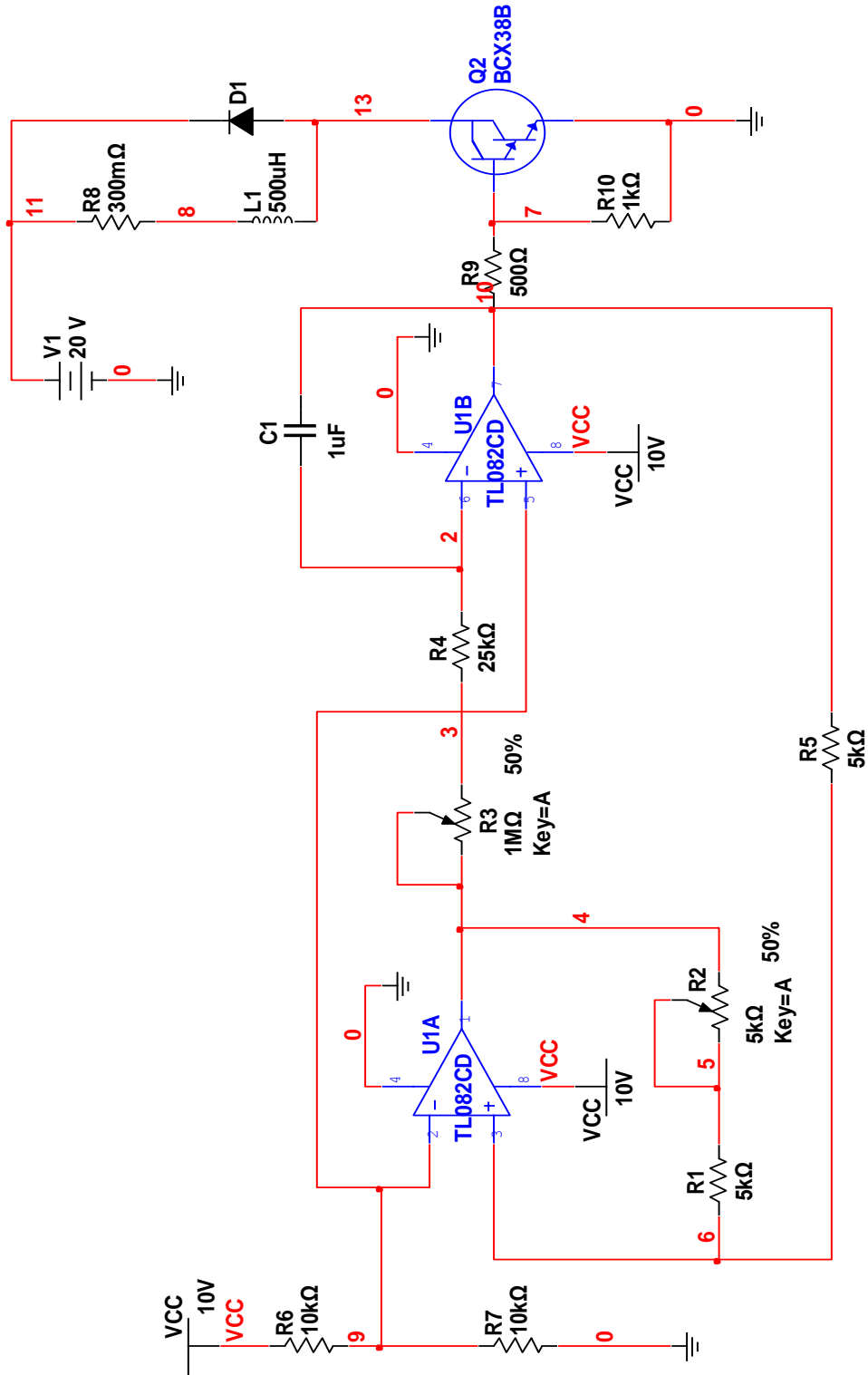
The results of each individual module concluded that the system worked as desired. The results of the overall circuit modules were very promising as it was previously shown. The overall results for the dynamic electromagnetic suspension system designed indicated that the vehicles body will stay at the same vertical position at all times regardless of the road conditions. It is clear that an important phase in the design of new generation suspension system was accomplished. This design however has to go through many phases before it can be implemented in actual vehicles.

9. Bibliography

1. **S. Mirzaei, S.M. Saghaiannejad, V. Tahani and M. Moallem.** Electromagnetic Shock Absorber. *IEEEEXPLORE*. [Online] 2001. [Cited: March 17, 2009.] <http://ieeexplore.ieee.org/stamp/stamp.jsp?arnumber=00939401>.
2. **Shock_Absorbers.** Types of Shock Absorbers. *Shock Absorbers B2B Marketplace*. [Online] [Cited: February Thursday, 2009.] <http://www.shockabsorbersworld.com/shock-absorber-types.html>.
3. **Maxim_Innovation.** Digitally Controlled Sine Wave Generator. *Maxim Innovation Delivered Website*. [Online] June 27, 2003. [Cited: January 5, 2009.] http://www.maxim-ic.com/appnotes.cfm/an_pk/2081.
4. **National_Semiconductor.** TL082 Datasheet. *National Semiconductor*. [Online] November 1994. [Cited: January 5, 2009.] <http://www.datasheetcatalog.org/datasheet/nationalsemiconductor/DS008357.PDF>.
5. **Mak, Se-yuen.** Six Ways to Measure Inductance. *IOP Science*. [Online] September 2002. <http://iopscience.iop.org/0031-9120/37/5/411/pdf?ejredirect=.iopscience>.
6. **Mitsubishi_Electric.** QM50DY-2H Datasheet. *Datasheet Catalog Website*. [Online] February 1999. [Cited: Jan 5, 2009.] <http://www.datasheetcatalog.org/datasheet/MitsubishiElectricCorporation/mXuswys.pdf>.
7. **Dimmension_Engineering.** DE-ACCM3D Buffered 3D Accelerometer. *Dimmension Engineering*. [Online] 2000. [Cited: January 5, 2009.] <http://www.dimensionengineering.com/datasheets/DE-ACCM3D2.pdf>.
8. **National_Semiconductor.** LM555 Timer Datasheet. *National Semiconductor*. [Online] July 2006. [Cited: 03 15, 2009.] <http://www.national.com/ds/LM/LM555.pdf>.
9. **Superior_Electric.** Powerstat Transformer Instructions. *Superior Electric*. [Online] 2000. http://www.superiorelectric.com/PDF/z30pwst_instr_002105-006g.pdf.

10. **Bitar, Stephen J.** SCHMITT-TRIGGER RELAXATION OSCILLATOR. Worcester, MA, U.S.A : s.n., November 12, 2007.
11. **Mouser_Electronics.** 381N1MEG Datasheet. *Mouser Electronics*. [Online] [Cited: January 5, 2009.]
<http://www.mouser.com/Search/ProductDetail.aspx?qs=sGAEpiMZZMsEGgLEzQVydmFA560EN7E8RuD3qUFm7VY%3d>.
12. **Wikimedia_Commons.** BJT Symbol NPN. *Wikimedia Commons*. [Online] March 23, 2008. [Cited: March 10, 2009.]
http://commons.wikimedia.org/wiki/File:BJT_symbol_NPN.svg.
13. **Piclist.** Triangular Wave Oscillator. *PICLIST website*. [Online] 2009. [Cited: February 20, 2009.] http://www.piclist.com/images/www/hobby_elec/e_ckt16.htm.
14. **Arun, P.** *Electronics*. Oxford : Alpha Science Int'l Ltd, 2005.

APPENDIX A1: SCHEMATICS



ROAD CONTROLLER

APPENDIX B. PSPICE CODE

```

*****
* OPAMP MACRO MODEL, SINGLE-POLE *
* connections:      non-inverting input *
*                  |   inverting input *
*                  |   |   output      *
*                  |   |   |           *
.SUBCKT OPAMP      P   N   T1           ;*
Rin P   N 100MEG          ;*
Ea A  0 TABLE { V(P,N) } = 0,0  1u 10 1000,10 ;*
                                           ;*
Rc   A  T1 100           ;*
Co   T1  0 1000p        ;*
ROUT T1  0 10MEG        ;*
                                           ;*
.ENDS                                           ;*
*****

*-----
*****
* H-BRIDGE WITH DIODES CONNECTED ;*
                                           ;*
* CONNECTIONS:      POSITIVE TURMINAL ;*
*                  |   NEGATIVE TURMINAL ;*
*                  |   |   TRANSISTER 1 ;*
*                  |   |   |   TRANSISTER 2 ;*
*                  |   |   |   |   TRANSISTER 3 ;*
*                  |   |   |   |   |   TRANSITER 4 ;*
*                  |   |   |   |   |   |   ;*
*                  |   |   |   |   |   |   ;*
.SUBCKT H_BRIDGE  M1  M2  Y1  Y2  Y3  Y4 ;*
                                           ;*
S1  10  M1  Y1  0  PTR A ;*
S2  M1  0  Y2  0  PTR A ;*
S3  10  M2  Y3  0  PTR A ;*
S4  M2  0  Y4  0  PTR A ;*
                                           ;*
.MODEL PTR A VSWITCH (RON=1U ROFF=10MEG VON=.1) ;*
                                           ;*
** DIODE CONNECTIONS ;*
                                           ;*
DQA 0  M1  DIODE ;*
DQB M1  10  DIODE ;*
DQC 0  M2  DIODE ;*
DQD M2  10  DIODE ;*
.MODEL DIODE D(N=.0001 RS=2U BV=120000) ;*
                                           ;*
*DC VOLTAGE CONNECTED TO THE H-BRIGE ;*
CFILTER 10  0  10u ;*
VBIAS   10  0  6V ;*
.ENDS ;*
*****

*THIS SECTION WILL GENERATE PULSES FOR H BRIDGE

```

```

*-----
Vtriangle Triangle 0 PULSE(2.5V 10V 0s 0.365ms 0.365ms .001ps 0.73ms)
Voffset Offset 0 6.75V ;DC offset
Vcontrol Control Offset SIN(0V 3V 10Hz)
Xplus Control Triangle P_Plus OPAMP
Xneg Triangle Control P_minus OPAMP
Rplus P_plus 0 10MEG ;positive pulse output
Rneg P_minus 0 10MEG ;negative pulse output

```

*THIS SECTION CONNECTS THE H-BRIDGE

```

*-----
Xbridge M1 M2 P_Plus P_minus P_minus P_Plus H_BRIDGE
Lcoil M1 B1 0.5m
Rcoil B1 M2 0.3
*-----

```

```

.PROBE
.TRAN 500m 500m 0 10m
.END

```

CURRENT DRIVER

```

Suspension System
Vroad 1 0 SIN(0 1 20)
Ck1 1 2 0.000714285714
Lms 2 3 1.6
Rd1 3 4 10
Lmb 4 0 1.8
Ck2 4 5 0.000862068966
Rd2 5 6 15
Econtrol 6 0 Value={V(30)}

```

*Proportional Amplifier

```

E1p 10 0 value={I(Lmb)}
R1p 10 20 10k
R2p 20 30 4000K
X1p 0 20 30 OPAMP
R3p 30 0 100MEG

```

* OPAMP MACRO MODEL, SINGLE-POLE WITH 50V OUTPUT CLAMP

```

* Connections:      non-inverting input
*                   |   inverting input
*                   |   |   output
*                   |   |   |

```

```

.SUBCKT OPAMP      n   p   o

```

* INPUT IMPEDANCE

```

RIN  n   p   10MEG
* DC GAIN=100K AND POLE1=100HZ
* UNITY GAIN = DCGAIN X POLE1 = 10MHZ

```

```

EGAIN a 0   n p   100K
RP1  a   b   100K
CP1  b   0   0.0159UF

```

* ZENER LIMITER

```

D1  b   d   DZ
D2  0   d   DZ

```

* OUTPUT BUFFER AND RESISTANCE

```

EBUFFER  c 0   b 0   1
ROUT  c o   10

```

```

*
.MODEL DZ D(Is=0.05u Rs=0.1 Bv=50 Ibv=0.05u)
.ENDS

```

.PROBE

```

.TRAN 500m 500m 0 1m
.END

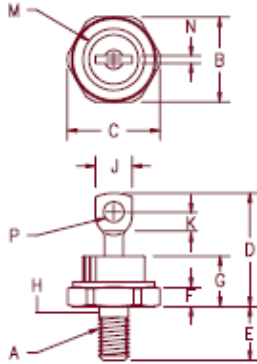
```

CONTROLLER PSPICE CODE

APPENDIX C: DATASHEETS

1N3766 DATASHEET.

Silicon Power Rectifier 1N1183–1N1190, 1N3765–1N3768



- Notes:
1. Full threads within 2 1/2 threads
 2. Standard Polarity: Stud is Cathode
Reverse Polarity: Stud is Anode

Dim.	Inches		Millimeter		Notes
	Minimum	Maximum	Minimum	Maximum	
A	----	----	----	----	1/4–28
B	.667	.687	16.95	17.44	
C	----	.793	----	20.14	
D	----	1.00	----	25.40	
E	.422	.453	10.72	11.50	
F	.115	.200	2.92	5.08	
G	----	.450	----	11.43	
H	.220	.249	5.59	6.32	1
J	.250	.375	6.35	9.52	
K	.156	----	3.97	----	
M	----	.667	----	16.94	Dia
N	----	.080	----	2.03	
P	.140	.175	3.56	4.44	Dia

D0203AB (D0–5)

JEDEC Numbers	Peak Reverse Voltage
1N1183, 1N1183A	50V
1N1184, 1N1184A	100V
1N1185, 1N1185A	150V
1N1186, 1N1186A	200V
1N1187, 1N1187A	300V
1N1188, 1N1188A	400V
1N1189, 1N1189A	500V
1N1190, 1N1190A	600V
1N3765	700V
1N3766	800V
1N3767	900V
1N3768	1000V

For Reverse Polarity add R to Part Number

- Glass Passivated Die
- 800A surge rating
- Glass to metal construction
- V_{RRM} to 1000V

Electrical Characteristics

Average forward current	$I_F(AV)$ 40 Amps	$T_C = 146^\circ C$, half sine wave, $R_{\theta JC} = 1.25^\circ C/W$
Maximum surge current	I_{FSM} 800 Amps	8.3ms, half sine, $T_J = 200^\circ C$
Max $I^2 t$ for fusing	$I^2 t$ 2600 A ² s	
Max peak forward voltage	V_{FM} 1.19 Volts	$I_{FM} = 90A; T_J = 25^\circ C^*$
Max peak reverse current	I_{RM} 10 μA	$V_{RRM, T_J} = 25^\circ C$
Max peak reverse current	I_{RM} 2.0 mA	$V_{RRM, T_J} = 150^\circ C$
Max Recommended Operating Frequency	10kHz	

*Pulse test: Pulse width 300 μ sec. Duty cycle 2%

Thermal and Mechanical Characteristics

Storage temperature range	T_{STG}	$-65^\circ C$ to $200^\circ C$
Operating junction temp range	T_J	$-65^\circ C$ to $200^\circ C$
Maximum thermal resistance	$R_{\theta JC}$	1.25 $^\circ C/W$ Junction to Case
Mounting torque		25–30 inch pounds
Weight		.5 ounces (14 grams) typical

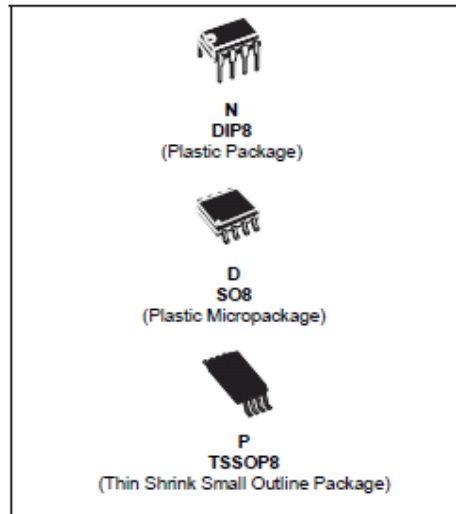
9–3–03 Rev. 1



TL082
TL082A - TL082B

**GENERAL PURPOSE J-FET
DUAL OPERATIONAL AMPLIFIERS**

- WIDE COMMON-MODE (UP TO V_{CC}^+) AND DIFFERENTIAL VOLTAGE RANGE
- LOW INPUT BIAS AND OFFSET CURRENT
- OUTPUT SHORT-CIRCUIT PROTECTION
- HIGH INPUT IMPEDANCE J-FET INPUT STAGE
- INTERNAL FREQUENCY COMPENSATION
- LATCH UP FREE OPERATION
- HIGH SLEW RATE : $16V/\mu s$ (typ)



DESCRIPTION

The TL082, TL082A and TL082B are high speed J-FET input dual operational amplifiers incorporating well matched, high voltage J-FET and bipolar transistors in a monolithic integrated circuit.

The devices feature high slew rates, low input bias and offset current, and low offset voltage temperature coefficient.

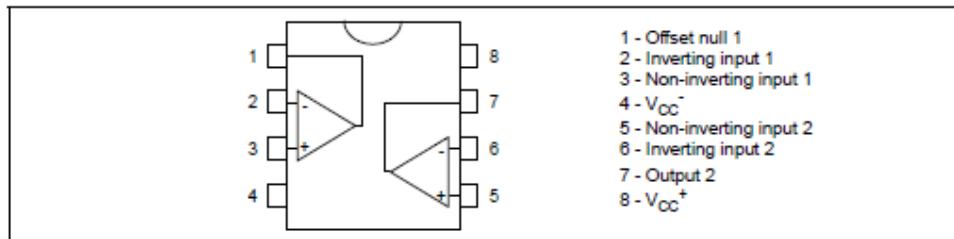
ORDER CODE

Part Number	Temperature Range	Package		
		N	D	P
TL082M/AM/BM	-55°C, +125°C	•	•	•
TL082I/AI/BI	-40°C, +105°C	•	•	•
TL082C/AC/BC	0°C, +70°C	•	•	•

Example : TL082CD, TL082IN

N = Dual In Line Package (DIP)
D = Small Outline Package (SO) - also available in Tape & Reel (DT)
P = Thin Shrink Small Outline Package (TSSOP) - only available in Tape & Reel (PT)

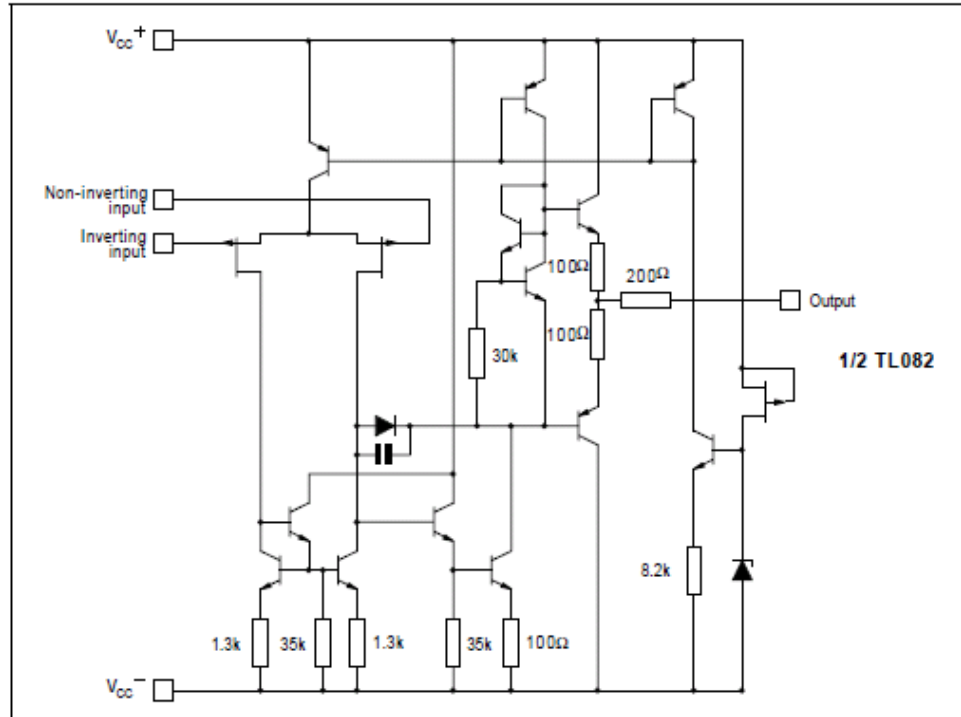
PIN CONNECTIONS (top view)



March 2002

1/11

SCHEMATIC DIAGRAM



ABSOLUTE MAXIMUM RATINGS

Symbol	Parameter	TL082M, AM, BM	TL082I, AI, BI	TL082C, AC, BC	Unit
V_{CC}	Supply voltage - note 1)	±18			V
V_I	Input Voltage - note 2)	±15			V
V_{Id}	Differential Input Voltage - note 3)	±30			V
P_{tot}	Power Dissipation	680			mW
	Output Short-circuit Duration - note 4)	Infinite			
T_{oper}	Operating Free-air Temperature Range	-55 to +125	-40 to +105	0 to +70	°C
T_{stg}	Storage Temperature Range	-65 to +150			°C

1. All voltage values, except differential voltage, are with respect to the zero reference level (ground) of the supply voltages where the zero reference level is the midpoint between V_{CC}^+ and V_{CC}^- .
2. The magnitude of the input voltage must never exceed the magnitude of the supply voltage or 15 volts, whichever is less.
3. Differential voltages are the non-inverting input terminal with respect to the inverting input terminal.
4. The output may be shorted to ground or to either supply. Temperature and/or supply voltages must be limited to ensure that the dissipation rating is not exceeded.

ELECTRICAL CHARACTERISTICS

$V_{CC} = \pm 15V$, $T_{amb} = +25^{\circ}C$ (unless otherwise specified)

Symbol	Parameter	TL082I,M,AC,AI,AM, BC,BI,BM			TL082C			Unit
		Min.	Typ.	Max.	Min.	Typ.	Max.	
V_{IO}	Input Offset Voltage ($R_G = 50\Omega$) $T_{amb} = +25^{\circ}C$		3	10		3	10	mV
	$T_{min} \leq T_{amb} \leq T_{max}$		1	3 13 7 5			13	
DV_{IO}	Input Offset Voltage Drift		10			10		$\mu V/^{\circ}C$
I_{IO}	Input Offset Current - note 1) $T_{amb} = +25^{\circ}C$		5	100		5	100	pA nA
	$T_{min} \leq T_{amb} \leq T_{max}$			4			10	
I_{IB}	Input Bias Current -note 1 $T_{amb} = +25^{\circ}C$		20	200		20	400	pA nA
	$T_{min} \leq T_{amb} \leq T_{max}$			20			20	
A_{vd}	Large Signal Voltage Gain ($R_L = 2k\Omega$, $V_O = \pm 10V$) $T_{amb} = +25^{\circ}C$	50	200		25	200		V/mV
	$T_{min} \leq T_{amb} \leq T_{max}$	25			15			
SVR	Supply Voltage Rejection Ratio ($R_G = 50\Omega$) $T_{amb} = +25^{\circ}C$	80	86		70	86		dB
	$T_{min} \leq T_{amb} \leq T_{max}$	80			70			
I_{CC}	Supply Current, no load $T_{amb} = +25^{\circ}C$		1.4	2.5		1.4	2.5	mA
	$T_{min} \leq T_{amb} \leq T_{max}$			2.5			2.5	
V_{ICM}	Input Common Mode Voltage Range	± 11	+15 -12		± 11	+15 -12		V
CMR	Common Mode Rejection Ratio ($R_G = 50\Omega$) $T_{amb} = +25^{\circ}C$	80	86		70	86		dB
	$T_{min} \leq T_{amb} \leq T_{max}$	80			70			
I_{OS}	Output Short-circuit Current $T_{amb} = +25^{\circ}C$	10	40	60	10	40	60	mA
	$T_{min} \leq T_{amb} \leq T_{max}$	10		60	10		60	
$\pm V_{OPP}$	Output Voltage Swing $T_{amb} = +25^{\circ}C$							V
	$R_L = 2k\Omega$	10	12		10	12		
	$R_L = 10k\Omega$	12	13.5		12	13.5		
	$T_{min} \leq T_{amb} \leq T_{max}$							
SR	Slew Rate ($T_{amb} = +25^{\circ}C$) $V_{in} = 10V$, $R_L = 2k\Omega$, $C_L = 100pF$, unity gain	8	16		8	16		V/ μs
t_r	Rise Time ($T_{amb} = +25^{\circ}C$) $V_{in} = 20mV$, $R_L = 2k\Omega$, $C_L = 100pF$, unity gain		0.1			0.1		μs
K_{OV}	Overshoot ($T_{amb} = +25^{\circ}C$) $V_{in} = 20mV$, $R_L = 2k\Omega$, $C_L = 100pF$, unity gain		10			10		%
GBP	Gain Bandwidth Product ($T_{amb} = +25^{\circ}C$) $V_{in} = 10mV$, $R_L = 2k\Omega$, $C_L = 100pF$, $f = 100kHz$	2.5	4		2.5	4		MHz
R_i	Input Resistance		10^{12}			10^{12}		Ω



LM348 DATASHEET

LM148, LM248, LM348 QUADRUPLE OPERATIONAL AMPLIFIERS

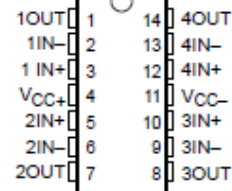
SLOS058C – OCTOBER 1979 – REVISED DECEMBER 2002

- μ A741 Operating Characteristics
- Low Supply-Current Drain . . . 0.6 mA Typ (per amplifier)
- Low Input Offset Voltage
- Low Input Offset Current
- Class AB Output Stage
- Input/Output Overload Protection
- Designed to Be Interchangeable With Industry Standard LM148, LM248, and LM348

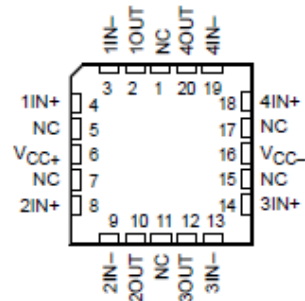
description/ordering information

The LM148, LM248, and LM348 are quadruple, independent, high-gain, internally compensated operational amplifiers designed to have operating characteristics similar to the μ A741. These amplifiers exhibit low supply-current drain and input bias and offset currents that are much less than those of the μ A741.

LM148 . . . J PACKAGE
LM248 . . . D OR N PACKAGE
LM348 . . . D, N, OR NS PACKAGE
(TOP VIEW)



LM148 . . . FK PACKAGE
(TOP VIEW)



NC – No internal connection

ORDERING INFORMATION

T_A	$V_{IO,max}$ AT 25°C	PACKAGE†	ORDERABLE PART NUMBER	TOP-SIDE MARKING
0°C to 70°C	6 mV	PDIP (N)	Tube of 25	LM348N
		SOIC (D)	Tube of 50	LM348D
			Reel of 2500	LM348DR
		SOP (NS)	Reel of 2000	LM348NSR
–25°C to 85°C	6 mV	PDIP (N)	Tube of 25	LM248N
		SOIC (D)	Tube of 50	LM248D
			Reel of 2500	LM248DR
		CDIP (J)	Tube of 25	LM148J
–55°C to 125°C	5 mV	LCCC (FK)	Tube of 50	LM148FK

† Package drawings, standard packing quantities, thermal data, symbolization, and PCB design guidelines are available at www.ti.com/sc/package.



Please be aware that an important notice concerning availability, standard warranty, and use in critical applications of Texas Instruments semiconductor products and disclaimers thereto appears at the end of this data sheet.

PRODUCTION DATA Information is current as of publication date. Products conform to specifications per the terms of Texas Instruments standard warranty. Production processing does not necessarily include testing of all parameters.

**TEXAS
INSTRUMENTS**

POST OFFICE BOX 655303 • DALLAS, TEXAS 75265

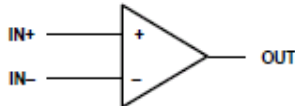
Copyright © 2002, Texas Instruments Incorporated
On products compliant to MIL-PRF-38535, all parameters are tested unless otherwise noted. On all other products, production processing does not necessarily include testing of all parameters.

1

LM148, LM248, LM348 QUADRUPLE OPERATIONAL AMPLIFIERS

SLOS058C – OCTOBER 1979 – REVISED DECEMBER 2002

symbol (each amplifier)



absolute maximum ratings over operating free-air temperature range (unless otherwise noted)[†]

Supply voltage, V_{CC+} (see Note 1):	LM148	22 V
	LM248, LM348	18 V
Supply voltage, V_{CC-} (see Note 1):	LM148	-22 V
	LM248, LM348	-18 V
Differential input voltage, V_{ID} (see Note 2):	LM148	44 V
	LM248, LM348	36 V
Input voltage, V_I (either input, see Notes 1 and 3):	LM148	-22 V
	LM248, LM348	-18 V
Duration of output short circuit (see Note 4)		Unlimited
Operating virtual junction temperature, T_J		150°C
Package thermal impedance, θ_{JA} (see Notes 5 and 6):	D package	86°C/W
	N package	80°C/W
	NS package	76°C/W
Package thermal impedance, θ_{JC} (see Notes 7 and 8):	FK package	5.61°C/W
	J package	15.05°C/W
Case temperature for 60 seconds: FK package		260°C
Lead temperature 1,6 mm (1/16 inch) from case for 10 seconds: J package		300°C
Lead temperature 1,6 mm (1/16 inch) from case for 60 seconds: D, N, or NS package		260°C
Storage temperature range, T_{stg}		-65°C to 150°C

[†] Stresses beyond those listed under "absolute maximum ratings" may cause permanent damage to the device. These are stress ratings only, and functional operation of the device at these or any other conditions beyond those indicated under "recommended operating conditions" is not implied. Exposure to absolute-maximum-rated conditions for extended periods may affect device reliability.

- NOTES:
- All voltage values, unless otherwise noted, are with respect to the midpoint between V_{CC+} and V_{CC-} .
 - Differential voltages are at IN+ with respect to IN-.
 - The magnitude of the input voltage must never exceed the magnitude of the supply voltage or the value specified in the table, whichever is less.
 - The output may be shorted to ground or either power supply. Temperature and/or supply voltages must be limited to ensure that the dissipation rating is not exceeded.
 - Maximum power dissipation is a function of $T_J(\max)$, θ_{JA} , and T_A . The maximum allowable power dissipation at any allowable ambient temperature is $P_D = (T_J(\max) - T_A)/\theta_{JA}$. Operating at the absolute maximum T_J of 150°C can affect reliability.
 - The package thermal impedance is calculated in accordance with JESD 51-7.
 - Maximum power dissipation is a function of $T_J(\max)$, θ_{JC} , and T_C . The maximum allowable power dissipation at any allowable ambient temperature is $P_D = (T_J(\max) - T_C)/\theta_{JC}$. Operating at the absolute maximum T_J of 150°C can affect reliability.
 - The package thermal impedance is calculated in accordance with MIL-STD-883.

recommended operating conditions

	MIN	MAX	UNIT
Supply voltage, V_{CC+}	4	18	V
Supply voltage, V_{CC-}	-4	-18	V

LM148, LM248, LM348
 QUADRUPLE OPERATIONAL AMPLIFIERS

SLOS058C – OCTOBER 1979 – REVISED FEBRUARY 2002

electrical characteristics at specified free-air temperature, $V_{CC\pm} = \pm 15$ V (unless otherwise noted)

PARAMETER	TEST CONDITIONS†	LM148			LM248			LM348			UNIT
		MIN	TYP	MAX	MIN	TYP	MAX	MIN	TYP	MAX	
V_{IO}	Input offset voltage										
			$V_O = 0$								
				25°C	1	5	6	1	6	1	6
				Full range							
				25°C	4	25	6	4	25	4	50
I_{IO}	Input offset current		$V_O = 0$								
				Full range							
				25°C	30	100	75	30	125	30	100
I_{IB}	Input bias current		$V_O = 0$								
				Full range							
				25°C	30	100	325	30	200	30	200
V_{ICR}	Common-mode input voltage range		$V_O = 0$								
				Full range							
				25°C	±12	±13	±12	±12	±13	±12	±13
V_{OM}	Maximum peak output voltage swing		$R_L = 10$ k Ω								
				Full range							
				25°C	±10	±12	±12	±10	±12	±10	±12
				Full range							
				25°C	±10	±12	±12	±10	±12	±10	±12
A_{VD}	Large-signal differential voltage amplification		$V_O = \pm 10$ V, $R_L \geq 2$ k Ω								
				Full range							
				25°C	50	160	25	160	25	160	15
r_i	Input resistance†		$V_O = 0$								
				Full range							
				25°C	25	160	15	160	15	160	15
B_1	Unity-gain bandwidth		$A_{VD} = 1$								
				Full range							
				25°C	0.8	2.5	0.8	2.5	0.8	2.5	0.8
ϕ_m	Phase margin		$A_{VD} = 1$								
				Full range							
				25°C	60°	60°	60°	60°	60°	60°	60°
CMRR	Common-mode rejection ratio		$V_{IC} = V_{ICRmin}$, $V_O = 0$								
				Full range							
				25°C	70	90	70	90	70	90	70
kSVR	Supply-voltage rejection ratio ($\Delta V_{CC\pm}/\Delta V_{IO}$)		$V_{CC\pm} = \pm 6$ V to ± 15 V, $V_O = 0$								
				Full range							
				25°C	77	96	77	96	77	96	77
IOS	Short-circuit output current		$V_O = 0$								
				Full range							
				25°C	±25	±25	±25	±25	±25	±25	±25
I _{CC}	Supply current (four amplifiers)		No load								
				Full range							
				25°C	2.4	3.6	2.4	4.5	2.4	4.5	2.4
V_{O1}/V_{O2}	Crosstalk attenuation		$f = 1$ Hz to 20 kHz								
				Full range							
				25°C	120	120	120	120	120	120	120

† All characteristics are measured under open-loop conditions with zero common-mode input voltage, unless otherwise specified. Full range for T_A is -55°C to 125°C for LM148, -25°C to 85°C for LM248, and 0°C to 70°C for LM348.
 ‡ This parameter is not production tested.



POST OFFICE BOX 655303 • DALLAS, TEXAS 75265

MITSUBISHI TRANSISTOR MODULES

QM50DY-2H

MEDIUM POWER SWITCHING USE
INSULATED TYPE

QM50DY-2H



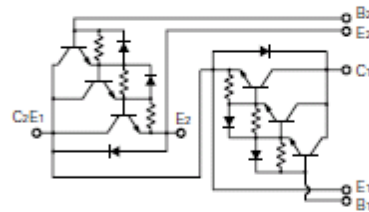
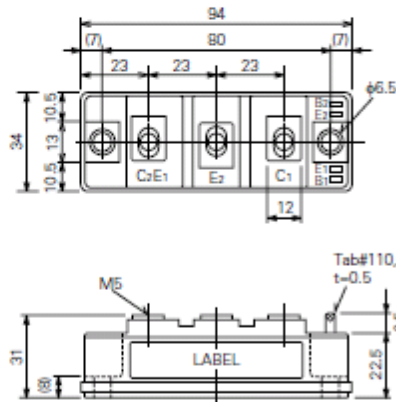
- **IC** Collector current **50A**
- **VCEX** Collector-emitter voltage **1000V**
- **hFE** DC current gain **75**
- **Insulated Type**
- **UL Recognized**
Yellow Card No. E80276 (N)
File No. E80271

APPLICATION

Inverters, Servo drives, UPS, DC motor controllers, NC equipment, Welders

OUTLINE DRAWING & CIRCUIT DIAGRAM

Dimensions in mm



Feb.1999



MITSUBISHI TRANSISTOR MODULES

QM50DY-2H

MEDIUM POWER SWITCHING USE
INSULATED TYPE

ABSOLUTE MAXIMUM RATINGS (T_J=25°C, unless otherwise noted)

Symbol	Parameter	Conditions	Rating	Unit
V _{CE(sus)}	Collector-emitter voltage	I _C =1A, V _{BE} =2V	1000	V
V _{CE}	Collector-emitter voltage	V _{BE} =2V	1000	V
V _{CB}	Collector-base voltage	Emitter open	1000	V
V _{BE}	Emitter-base voltage	Collector open	7	V
I _C	Collector current	DC	50	A
-I _C	Collector reverse current	DC (forward diode current)	50	A
P _C	Collector dissipation	T _C =25°C	400	W
I _B	Base current	DC	3	A
-I _{CSM}	Surge collector reverse current (forward diode current)	Peak value of one cycle of 60Hz (half wave)	500	A
T _J	Junction temperature		-40-+150	°C
T _{stg}	Storage temperature		-40-+125	°C
V _{iso}	Isolation voltage	Charged part to case, AC for 1 minute	2500	V
—	Mounting torque	Main terminal screw M5	1.47-1.96	N·m
			15-20	kg·cm
		Mounting screw M6	1.96-2.94	N·m
			20-30	kg·cm
—	Weight	Typical value	210	g

ELECTRICAL CHARACTERISTICS (T_J=25°C, unless otherwise noted)

Symbol	Parameter	Test conditions	Limits			Unit
			Min.	Typ.	Max.	
I _{CX}	Collector cutoff current	V _{CE} =1000V, V _{BE} =2V	—	—	1.0	mA
I _{CB}	Collector cutoff current	V _{CB} =1000V, Emitter open	—	—	1.0	mA
I _{EB}	Emitter cutoff current	V _{BE} =7V	—	—	200	mA
V _{CE(sat)}	Collector-emitter saturation voltage	I _C =50A, I _B =1A	—	—	2.5	V
V _{BE(sat)}	Base-emitter saturation voltage		—	—	3.5	V
-V _{CEO}	Collector-emitter reverse voltage	-I _C =50A (diode forward voltage)	—	—	1.8	V
h _{FE}	DC current gain	I _C =50A, V _{CE} =2.8V/5V	75/100	—	—	—
t _{on}	Switching time	V _{CE} =600V, I _C =50A, I _B =-I _{BE} =1A	—	—	2.5	μs
t _s			—	—	15	μs
t _f			—	—	3.0	μs
R _{th(j-c)}	Thermal resistance (junction to case)	Transistor part (per 1/2 module)	—	—	0.31	°C/W
R _{th(j-d)}		Diode part (per 1/2 module)	—	—	1.2	°C/W
R _{th(c-f)}	Contact thermal resistance (case to fin)	Conductive grease applied (per 1/2 module)	—	—	0.15	°C/W

Feb.1999



QM50DY-2H

MEDIUM POWER SWITCHING USE
INSULATED TYPE

PERFORMANCE CURVES

